A Stand-Alone Adaptive Corrosion Protection System (ACPS) in Various Corrosive Environments

by

Yogiraj Kachhela

B.A.Sc, University of British Columbia (Vancouver), 2018

Thesis Submitted in Partial Fulfillment of the
Requirements for the Degree of
Master of Applied Science

in the
School of Engineering Science
Faculty of Applied Sciences

SIMON FRASER UNIVERSITY
Summer 2019

Approval

Name:	**Yogiraj Kachhela**
Degree:	**Master of Applied Science**
Title:	**A Stand-Alone Adaptive Corrosion Protection System (ACPS) in Various Corrosive Environments**

Examining Committee:

Chair: **Shahram Payandeh**
Professor

Bozena Kaminska
Senior Supervisor
Professor

Anita Tino
Supervisor
Lecturer

Andrew Rawicz
Internal Examiner
Professor

Date Defended/Approved: July 26, 2019

Abstract

A novel approach to corrosion monitoring and protection is investigated in different corrosive environments. The standalone Adaptive Corrosion Protection System (ACPS) works in a feedback loop to monitor the corrosion status and protect the target metal. Experiments in different corrosive mediums are carried out using a new stand-alone ACPS unit. A comparative study of the ACPS with the standard Impressed Current Cathodic Protection (ICCP) is done in corrosive mediums at different temperatures and pH. Furthermore, a miniature transmission tower grillage structure buried in the soil is protected using the ACPS. The variations of the electrochemical parameters in different environments are studied and correlated with the macro-environment data. Dynamic ACPS can optimize power consumption by updating the protection parameters at a user-defined interval. Unlike the standard ICCP, the adaptive corrosion protection mechanism is a current-sourced system that effectively monitors and optimally protects the target structure.

Keywords: corrosion; cathodic protection; corrosion monitoring; protection efficiency; environmental corrosion

I pay my sincere tribute to Bhagwan Swaminarayan, Guru Pramukh Swami Maharaj and Mahant Swami Maharaj

I dedicate the chapters of this enterprise to my parents

Acknowledgements

I am thankful to my senior supervisor Dr. Bozena Kaminska and my advisor Dr. Jasbir Patel for their unwavering support and guidance during the process. Their expertise, valuable insights and scientific rigour have steered me in the right direction. They constantly motivated me to learn not only the topics related to the field of my research but, also helped me to grasp matters related to finance, project management and industrial liaison. In addition, I am grateful to my supervisory and examining committee members Dr. Andrew Rawicz and Dr. Anita Tino to review and approve my work.

I am appreciative to Lana Gilpin-Jackson, Giuseppe Stanciulescu, Earl Mayuga, Patrick Ho and Sid Cherukupalli from BC Hydro and Powertech Labs for their support and technical guidance. Additionally, I acknowledge the support from Mitacs, Powertech Labs and BC Hydro to carry out this experimental work at the Simon Fraser University in Burnaby, British Columbia.

I would also like to thank the School of Engineering Science faculty staff for their support. I acknowledge the contribution of co-op students for this project.

This accomplishment would not have been possible without the support and involvement from all. Thank you!

Author

Yogiraj Kachhela

Table of Contents

List of Tables

List of Figures

List of Acronyms

ACPS	Adaptive Corrosion Protection System
AWWA	American Water Works Association
$CaCl_2$	Calcium Chloride
CE	Counter Electrode
CP	Cathodic Protection
EIS	Electrochemical Impedance Spectroscopy
GUI	Graphic User Interface
H_2SO_4	Sulphuric Acid
ICCP	Impressed Current Cathodic Protection
IMPACT	International Measures of Prevention, Application, and Economics of Corrosion Technologies
IPA	Isopropyl Alcohol
KCl	Potassium Chloride
KNO_3	Potassium Nitrate
$MgSO_4$	Magnesium Sulfate
Na_2SO_4	Sodium Sulfate
NACE	National Association of Corrosion Engineers
NaCl	Sodium Chloride
$NaHCO_3$	Sodium Bicarbonate
NaOH	Sodium Hydroxide
OCP	Open Circuit Potential
RE	Reference Electrode
SCE	Standard Calomel Electrode
SFU	Simon Fraser University
SHE	Standard Hydrogen Electrode
WE	Working Electrode

Preface

This research work is part of an ongoing research project at Simon Fraser University in collaboration with BC Hydro and Powertech Labs. BC Hydro being a crown corporation is authorized for generating and distributing electricity in the province of British Columbia (Canada). Additionally, Powertech Labs Inc. is a subsidiary of BC Hydro and one of the largest research and development facilities in North America. Thus, the research presented in this thesis is solely aimed at electric transmission towers. However, conceptually this work can be applied to various infrastructures.

The electric transmission towers are generally made of steel. The underground section (grillage) of the electric power transmission tower experiences degradation over time due to its interaction with the environment. Corrosion is a common problem in the utility industry. The problem of metal deterioration is further complicated by the diversity of environmental factors. To ensure the safety and reliability of the infrastructures, various protection measures are implemented. Among these time-proven methods, the most commonly used mechanism is the cathodic protection.

Several cathodic protection techniques have been implemented in different environments and studied over decades. A novel dynamic approach is used for this research. A feedback-loop based Adaptive Corrosion Protection System (ACPS) is used to protect the target metal in different environments.

A stand-alone ACPS module that works using grid power and off-grid solar energy is developed. The protection efficiency of the ACPS is compared with the commonly used standard Impressed Current Cathodic Protection (ICCP) method. A systematic experimental approach is taken to compare two systems in different temperatures and pH. Apart from experiments in the controlled environment, a miniature underground section (grillage) of the transmission tower is submerged in soil and the ACPS module is used to protect it. Macro-environment weather data (precipitation and temperature) is correlated with the electrochemical parameters of the ACPS.

The development of the research project stated in this dissertation will be used towards an in-field implementation of the standalone ACPS for the effective corrosion monitoring and protection. The module prepared for this research will be used to protect

the BC Hydro transmission tower grillage at the Powertech test facility in Surrey, British Columbia.

The following are the scholarly contribution from the research work presented in this thesis:

- **Y. Kachhela**, J. Patel, L. Gilpin-Jackson, and B. Kaminska, “A Stand-Alone Adaptive Corrosion Protection System for Efficient Protection in Different Corrosive Environments”, submitted to International Journal of Corrosion (manuscript # 9638579).

- **Y. Kachhela**, J. Patel, and B. Kaminska, “Adaptive Corrosion Protection System For a Smart-Grid Application”, National Association of Corrosion Engineers (NACE) BC Section, Richmond, BC, Canada, April 2019.

- **Y.Kachhela**, J.Patel, and B.Kaminska, "Risk Management of Metal Structures Using Adaptive Corrosion Protection System," National Association of Corrosion Engineers (NACE) Corrosion Risk Management Conference, Houston, Texas, USA, June 2018

- **Y.Kachhela**, J.Patel, D.Patel and B.Kaminska, “Nanotechnology Solving Environmental Protection (Corrosion) and Cyber-Physical Security: A Smart Power-Grid Application,” BCTech Summit, Vancouver, BC, Canada, May 2018

Chapter 1.

Introduction

There have been significant studies in various parts of the world to estimate the cost of corrosion and its effect on a country's economy. National Association of Corrosion Engineers (NACE) IMPACT researchers studied publicly available data around the world and have revealed the global cost of corrosion is a shocking US$2.5 trillion [1]. Due to innovation and technology upgradation, transmission and distribution section of the electric power system will go through a radical change in the near future [2]. The aging infrastructure, reliability improvements, and growth in the energy sector attract major investments to the transmission and distribution sector of the utility industry [3]. Additionally, the degradation of public infrastructure and physical systems due to corrosion affects public safety. Thus, these costs are not so readily quantifiable. Despite the difficulty to enumerate the effects of corrosion, other indirect expenditure by delays, loss of productivity and environmental impact add to the horrendous effects. Therefore, mitigating corrosion is not only about saving money but it also increases the efficiency of natural resources [4]. The unparallel growth projection of infrastructures make degradation due to corrosion a significant area of concern. This presents challenges and economic opportunities for both public and private industries around the world.

The Canadian utility company for the province of British Columbia (BC Hydro) has 33 fully owned transmission lines [5]. Additionally, the power transmission network is supported by towers that pose some unique protection challenges. Electrical transmission tower is primarily composed of: (1) above ground assembly to support overhead conductor and (2) underground foundation (grillage) having mechanical load-bearing capacity that supports the tower. The underground foundation of the electrical transmission structure is shown in Figure 1. The primary cause of equipment degradation in electric power transmission and distribution lines is the underground corrosion [6]. Materials experience interactions with diverse environments. In fact, various environmental factors contribute to the corrosion process in distinct ways. Corrosion is described as the destructive phenomena that affects metal due to its interaction with the surroundings [7] [8]. Metal atoms are present as minerals or in general as chemical compounds in nature. It requires

energy to extract metal from its compounds. During the corrosion process, metal returns back to a similar chemical compound from which it was extracted. Thus, corrosion is also referred to as ‘extractive metallurgy in reverse’ [8]. The ion interaction at the interface of material leads to corrosion. This process involves multiple steps and the slowest step controls the rate of the overall reaction. Factors such as resistivity, exposure to electrolytes, humidity, temperature, and pH all play a key role in the rate at which the material will corrode [9] [10]. Corrosion can occur in many forms. Commonly, corrosion classification is done in two major categories: (1) uniform corrosion and (2) localized corrosion [11]. Some types of uniform and localized corrosion are shown in Table 1.

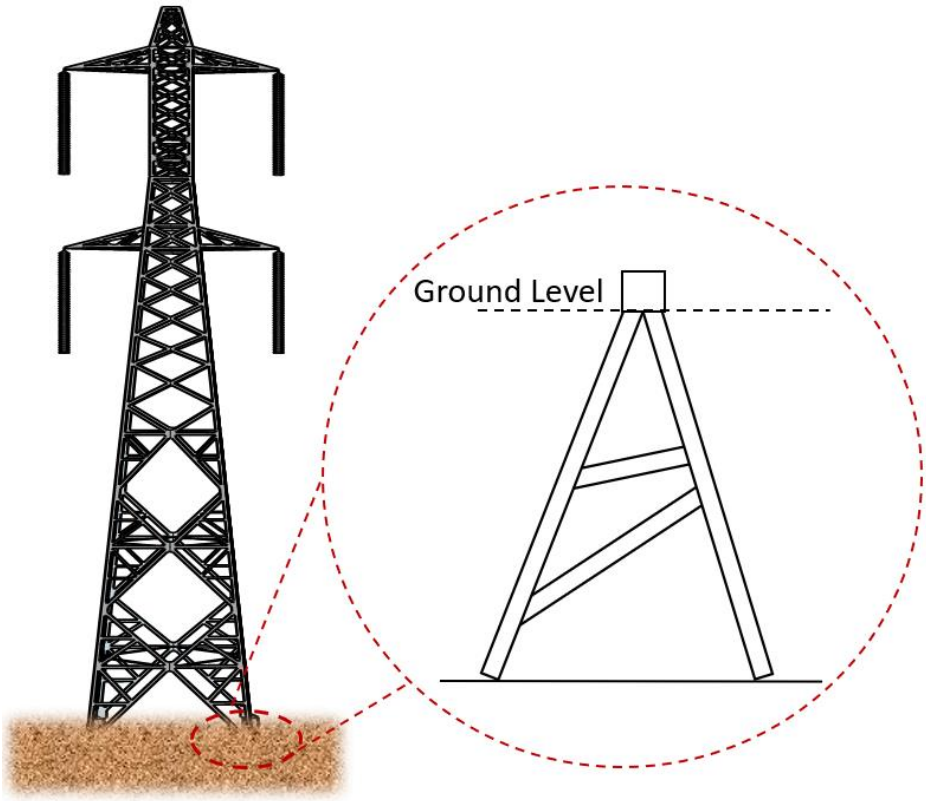

Figure 1: Underground foundation (grillage) of the electric transmission tower

Table 1: Various types of corrosion

Uniform Corrosion	Atmospheric, galvanic, stray-current etc.
Localized Corrosion	Crevice, filiform, biological and selective leaching etc.

The uniform degradation of metal throughout its surface area is referred to as uniform corrosion [8]. Atmospheric corrosion is the most common example of uniform corrosion. Consequently, for different kinds of corrosion, various protection techniques have been developed over the years. Material selection, cathodic protection, coatings, corrosion inhibitors, and condition control are some of the widely used methods for corrosion protection. These available, time-proven methods for preventing and controlling corrosion depend on the target metal and its environment. Cathodic Protection (CP) is proved to be an effective method for buried structures. CP is an electrochemical method to control the kinetics of the process by polarization [12]. CP methods are extensively used in the utility industry.

Underground structures are subject to aggressive corrosion and therefore protection practices need to be implemented. The grillage faces the risk of material degradation due to its interaction with the environment. Standard CP protocols for underground metallic systems are established by NACE [13]. Such protocols, although very useful, neglect the effects of changing environmental conditions. The aggressive soil environment, varying climatic conditions, stray currents, and microorganisms commence the process of corrosion [12]. Protection criteria are not optimized and cost-effective [6]. The focus of this study is to develop a standalone corrosion protection system using the proof-of-concept proposed by Patel et al. [14]. Additionally, emphasis is given to evaluate and validate the novel approach for effective corrosion protection in various corrosive environments. The proposed Adaptive Corrosion Protection System (ACPS) obtains an electrochemical response of the target metal. The protection parameters are extracted from the Tafel plot and are used to protect the target metal. The ACPS works in a closed-loop to monitor the corrosion status and optimize the protection parameters as required. It considers the interaction of the metal structure with its environment and hence provides a reliable and adaptive mechanism that optimally protects the target structure and negate the effects of under and over protection. It also offers cost savings by optimizing the energy requirements.

This adaptive, feedback-loop based mechanism is used for this dissertation in comparison with the NACE standard Impressed Current Cathodic Protection (ICCP). The comparison is conducted at different temperatures (3% saline solution) and pH (1N of HCl and NaOH). The temperature of the corrosive medium is varied from 30°C to 80°C and the pH is varied from 2 to 12 in this study. ASTM A36 metal coupons are used as the

target metal and weight-loss measurements are done to calculate the protection efficiency. Further, the standalone ACPS is used to protect miniature grillage structure submerged in the soil in an uncontrolled environment. The variation in protection parameters due to macro-environment factors (precipitation and temperature) is presented in this dissertation.

Thesis Outline

The study of the novel standalone Adaptive Corrosion Protection System (ACPS) in different corrosive environments is given in this dissertation. The feedback-loop based mechanism is effectively used to monitor and protect the target metal. The proceeding sections of this thesis contain:

- Background and Literature Review (Chapter 2): An overview of the background information of an electrochemical cell along with the standard cathodic protection practices is given in this section. Additionally, a review of various publications to study the effects of temperature and pH is presented. An in-depth literature study of soil corrosivity is also given. Finally, an overview of the novel ACPS mechanism is presented in this section.
- Objectives (Chapter 3): The goals of this extensive research are described in this section. The focus of the thesis that encompasses experimental study is highlighted. Key technical objectives present the contribution of this work to the ongoing research project at SFU.
- Preliminary Analysis (Chapter 4): A pilot research experiment using a simple LabView and Keithley based adaptive corrosion monitoring and protection mechanism is presented. A comparative analysis of ACPS with the widely used ICCP is carried out using saline solution at different temperatures.
- Corrosion Protection in Different Corrosive Environments (Chapter 5): A stand-alone ACPS module is developed for a systematic experimental study to protect the target metal in corrosive mediums at different temperatures and pH. The modular system is shown to work using off-grid solar energy. The results are compared with the standard ICCP system.
- Corrosion in Soil (Chapter 6): A miniature grillage structure is submerged in soil and is protected by modular ACPS. The extensive study is done in an uncontrolled

environment and the macro-environmental factors (precipitation and temperature) are correlated with the ACPS performance. This section presents the detailed experimental study and its results.

- Conclusions (Chapter 7): The summary of conclusions drawn from the experiments performed for this dissertation is given in this section. Relevant future recommendations are also presented.

Chapter 2.

Background and Literature Review

2.1. Electrochemical Cell

Corrosion is a chemical or electrochemical process that requires flow of the current [11]. Conductivity of the environment (referred as electrolyte) that enables electron transfer changes valency of the metal from zero to a positive value. Electrolytes contain positively charged cations and negatively charged anions. The overall reaction is made of two half-cell reactions that describe the electron transfer process at the two electrodes in an electrochemical cell [15]. The target metal is usually referred to as a working electrode (WE) and a counter electrode (CE) is a conductor to complete the cell circuit. These half-cell reactions can be described as either anodic or cathodic reactions. The third electrode in the electrochemical cell is the reference electrode (RE). The reference electrode has a fixed potential due to its constant makeup. Thus, the changes in the cell potential are ascribable to the working electrode [15]. The universally accepted primary reference is the standard hydrogen electrode (SHE) which has all components at a unit activity. For the corrosion reaction to occur, metal undergoes oxidation by transferring electrons to its environment ($M \rightarrow M^{m+} + me^{-}$). Consequently, the oxidation reaction is sustained by another reaction: $X^{x+} + xe^{-} \rightarrow X$. The basic corrosion process is shown in Figure 2. These electrochemical reactions occur at finite rates.

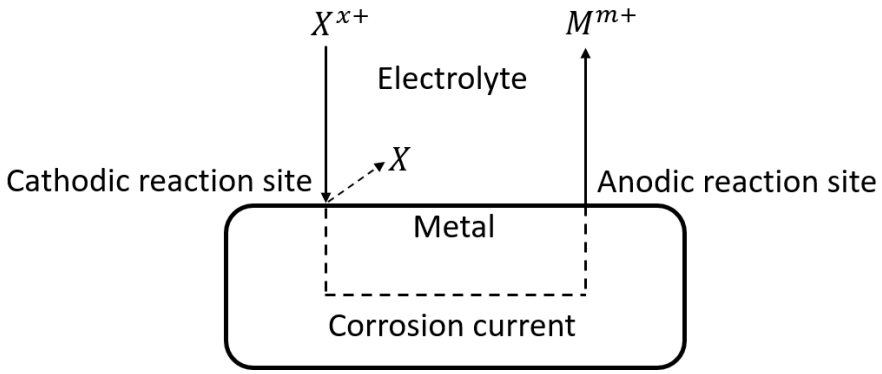

Figure 2: Flow of electrons in a basic corrosion process

An electrochemical system exhibits potential values relative to its reference. This is because the metal acts as a mixed electrode for two or more half-cell reactions. These electron transfer reactions occur on the metal surface. The position of the reference electrode along with the kinetics of the individual half-cell reactions contribute to the potential of the electrochemical system. The mass transfer due to the movement of electrons is given by the first law of electrolysis which is also known as Faraday's Law (Equation 1). The proportionality between mass transfer (m) in gram and the current (I) in Ampere can be used to calculate the corrosion rate (R). Mass transfer over time and surface area gives corrosion rate (R). Corrosion rate with relation to current density (i_{corr}) is given in Equation 2.

$$m = \frac{I \cdot t \cdot M}{n \cdot F} \tag{1}$$

$$R = \frac{m}{t \cdot A} = \frac{i_{corr} \cdot M}{n \cdot F} \tag{2}$$

When the electrochemical system is at equilibrium (half-cell reactions at equilibrium), the rate of forward and backward reaction is equal. At this point, the electrode potential can be stated as the reversible potential (E_{rev}). At potential values higher than this point (E_{rev}), oxidation occurs and for potential lower than E_{rev}, the reaction will proceed towards the reduction process. The exponential dependence of current on potential is shown in Figure 3.

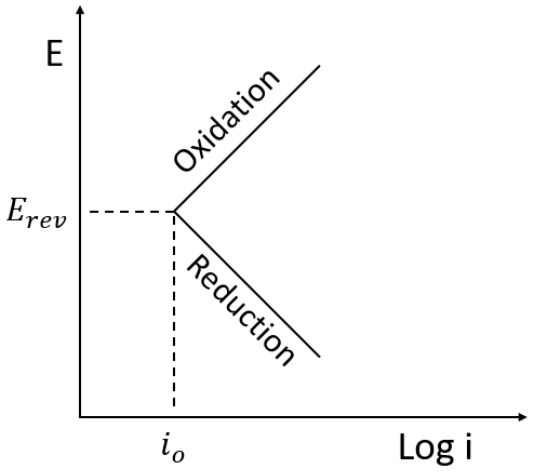

Figure 3: Exponential dependence of current on potential

The change in potential from the E_{rev}, is known as polarization. The reactions at the metal-electrolyte interface contribute to the activation polarization. The base of kinetic electrochemistry is given by the Butler-Volmer Equation (Equation 3). The Butler-Volmer equation states the relation of current density with the potential of the system undergoing activation control. The Evans Diagram (E log-I) plot shows the Tafel segment for the polarization curve. The straight lines (for sufficiently large potential) of the Tafel segment can be described by Tafel Equations [16] [17].

$$i = i_o \exp\left[\frac{\beta \cdot n \cdot F \cdot \eta}{RT}\right] - i_o \exp\left[\frac{-(1-\beta) \cdot n \cdot F \cdot \eta}{RT}\right] \quad (3)$$

Each half-cell reaction can proceed in both reduction and oxidation directions. During corrosion, the principle of charge conservation is stated in Equation 4. At the Open Circuit Potential (OCP), the sum of oxidation current must equal the sum of reduction current. Therefore, OCP is a mixed potential of oxidation and reduction. When the rate of hydrogen evolution equals the rate of metal dissolution (as shown in Figure 4), the potential is expressed by the corrosion potential (E_{corr}). The Tafel region is shown in Figure 5 [18].

$$\sum I_{oxd} = \sum I_{red} \quad (4)$$

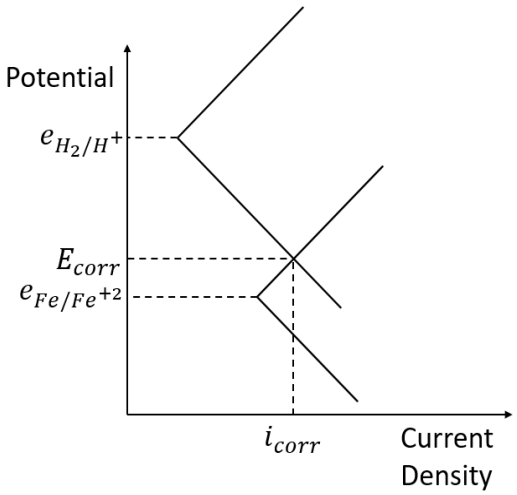

Figure 4: Mixed potential theory

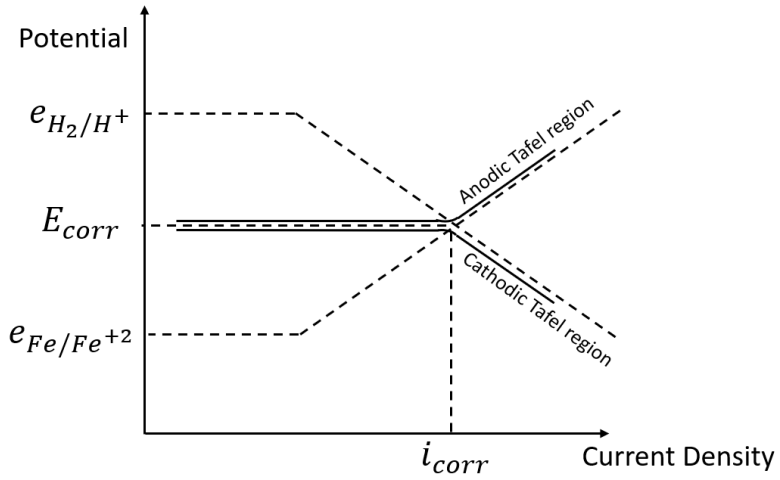

Figure 5: Polarization curve

2.2. Cathodic Protection

The protection mechanism for which the corrosion rate is decreased by cathodic polarization is referred as Cathodic Protection (CP). Hence, by making metal surface a cathode of an electrochemical process, this technique reduces corrosion of a metal surface [19]. It is an effective protection method widely used for various metallic structures such as storage tanks, pipelines, towers, etc [20]. NACE standard SP0169-2013 contains various cathodic protection criteria. These criteria are:

1. The minimum cathodic voltage of 0.85V with respect to the saturated copper-copper sulfate reference electrode.
2. The cathodic polarization voltage shift of 0.1V between the target metal and the reference electrode in an electrolyte.
3. The cathodic potential, which initially leads to the Tafel segment of the E-log-I curve.
4. The minimum cathodic voltage shift of 0.3V, produced by applying the protective current.
5. The net protective current applied to the structure from electrolyte that is measured by an earth current technique.

These criteria are widely adapted and used industrially. However, over the years, researchers have shown considerable disagreement between various cathodic protection criteria.

In 1933, Kuhn was the first researcher to state that the corrosion can be prevented if the potential is around -0.850V [21]. Since then numerous studies have been conducted for corrosion protection using this technique. This potential-based criterion described in NACE standard is often used to protect steel structures exposed to soil or water electrolytes [21]. The standard proposes the use of minimum cathodic voltage of 0.85V/CSE. One of the difficulties using this criterion is the requirement that the measurement be taken with the current applied [21]. Due to this, all measurements contain an IR drop error of unknown magnitude. Additionally, the changing environmental conditions (such as rain) alters the soil properties and magnify this effect. Hence, varying environmental factors affects the corrosion rate. Consequently, an adaptive corrosion protection system that considers the effect of environmental factors is needed. As infrastructures are generally composed of steel, numerous researches have been conducted to study the performance of steel under changing conditions [22] [23] [24] [25]. A review of some of these works is presented below.

2.3. Effect of Corrosive Environments

Several factors contribute to corrosion. Volumes of data have been accumulated to predict corrosion performance. Temperature and pH of the electrolyte contribute towards the degradation of the target metal. The importance of these factors cannot be disregarded for the corrosion process. Thus, this chapter presents a review of the effects of temperature and pH. Additionally, a study of corrosion performance of steel in soil with regards to multiple environmental factors is given in this section.

2.3.1. Effect of pH

Corrosion with respect to the electrode potential of the metal and pH of the solution is determined by the Pourbaix diagrams. These diagrams mark the zones of corrosion, immunity, and passivity based on the pH and the potential values [20]. Pourbaix diagrams are based on the Nernst Equation. These diagrams provide a thermodynamic knowledge to prevent corrosion by adjusting pH and/or potential. However, these diagrams do not

give any information about the kinetics of the process and therefore, cannot be used to determine the rate of the reaction. It only shows the thermodynamic tendency for the reaction to proceed.

Standard Gibbs Free Energy (ΔG°) shows the tendency of the reaction to proceed. The relation of the Standard Gibbs Free Energy with respect to the standard electrode potential is given in Equation 5, where n is the number of electrons per mole, F is the Faraday's constant and E° is the standard electrode potential. The force that drives the corrosion is the change in energy, namely Gibbs Free Energy. The energy change for an electrochemical reaction is given in Equation 6, where E is the electrochemical potential.

$$\Delta G^{\circ} = -nFE^{\circ} \tag{5}$$

$$\Delta G = \Delta G^{\circ} + nFE \tag{6}$$

When both products and reactants are present in equilibrium and have no further tendency to change, the forward and backward reaction rates are equal. Thus, the standard Gibbs Free Energy at equilibrium is given in Equation 7, where R is the universal gas constant, T is the absolute temperature and K is the equilibrium constant.

$$\Delta G^{\circ} = -RT \cdot Ln\left(K_{eq}\right) \tag{7}$$

Electrochemical reactions considered in the application are not usually in their standard states. The Nernst Equation (Equation 8) is the basis of the Porubaix diagram and accounts for the effect of the activity (α) on the potential (E).

$$E = E^{\circ} \frac{-RT}{nF} Ln\left[\frac{\left(\alpha_{products}\right)^{k}}{\left(\alpha_{reactants}\right)^{j}}\right] \tag{8}$$

Pourbaix diagram also known as the potential/pH diagram is specific to water for phases that are stable in an aqueous electrochemical system. Electrochemical equilibrium equation of hydrogen gas with an acid solution is shown in Equation 9a and with the neutral or alkaline solution is given in Equation 9b. Equation 9b is more appropriate at higher pH as OH^- is predominant over H^+. Relation of E_{rev} with respect to pH using the Nernst Equation is shown in Equation 10. For standard state, the relation of E_{rev} with respect to pH is shown in Equation 11.

$$2H^+ + 2e^- \rightarrow H_2(g) \tag{9a}$$

$$2H_2O + 2e^- \rightarrow H_2 + 2OH^- \tag{9b}$$

$$E_{rev\left(\frac{H^+}{H_2}\right)} = E^{\circ}_{\left(\frac{H^+}{H_2}\right)} - \frac{RT}{nF} \cdot Ln\left(\frac{[H_2]}{[H^+]^2}\right) \tag{10}$$

$$E_{rev\left(\frac{H^+}{H_2}\right)} = E^{\circ}_{\left(\frac{H^+}{H_2}\right)} - \frac{0.059}{2} \cdot Log([H^+]^2) = -0.059 \cdot pH \tag{11}$$

$where$: $E^{\circ}_{(H^+/H_2)} = 0$

$$Ln(x) \approx 2.3 \cdot Log(x)$$

$$\frac{2.3RT}{nF} = \frac{2.3(8.31\frac{J}{K \cdot mol})(298K)}{n\,(96485\frac{C}{eq \cdot e^-})} = 0.059V$$

$$pH = -\log(H^+)$$

Similarly, oxygen reduction reactions are given in Equation 12a for acids and Equation 12b for bases. Relation of E_{rev} with respect to pH is given in Equation 13.

$$O_2 + 4H^+ + 4e^- \rightarrow 2H_2O \tag{12a}$$

$$O_2 + 2H_2O + 4e^- \rightarrow 4OH^- \tag{12b}$$

$$E_{rev\left(\frac{O_2}{H_2O}\right)} = E^{\circ}_{\left(\frac{O_2}{H_2O}\right)} + \frac{0.059}{4} \cdot Log([H^+]^4) = 1.229 - 0.059 \cdot pH \tag{13}$$

Generally, infrastructure is made of cast iron and carbon steel [26]. Iron (Fe) has two oxidation states: $+2$ and $+3$. For usual conditions, iron equilibrium equations (Equation 14 to 18) are considered to construct a simple potential/pH diagram. The Pourbaix diagram of iron at 25°C is shown in Figure 6 and the lines are labeled according to the equation number. Values used for constructing this diagram are obtained from the literature and the stability lines on the Pourbaix diagram corresponds to the ionic activity of $10^{-6} g - equiv/L$ [8].

$$Fe = Fe^{+2} + 2e^- \tag{14a}$$

$$E_{rev} = -0.440 + 0.0295 \cdot Log([Fe^{+2}]) \tag{14b}$$

$$Fe + 2H_2O = HFeO_2^- + 3H^+ + 2e^- \quad (15a)$$

$$E_{rev} = 0.493 - 0.0886 \cdot pH + 0.0295 \cdot Log(HFeO_2^-) \quad (15b)$$

$$Fe^{+2} + 3H_2O = Fe(OH)_3 + 3H^+ + e^- \quad (16a)$$

$$E_{rev} = 1.057 - 0.1773 \cdot pH - 0.0591 \cdot Log(Fe^{+2}) \quad (16b)$$

$$Fe^{+3} + 3H_2O = Fe(OH)_3 + 3H^+ \quad (17a)$$

$$pH = 1.613 - \frac{1}{3} \cdot Log(Fe^{+3}) \quad (17b)$$

$$HFeO_2^- + H_2O = Fe(OH)_3 + 2e^- \quad (18a)$$

$$E_{rev} = -0.810 - 0.0591 \cdot Log(HFeO_2^-) \quad (18b)$$

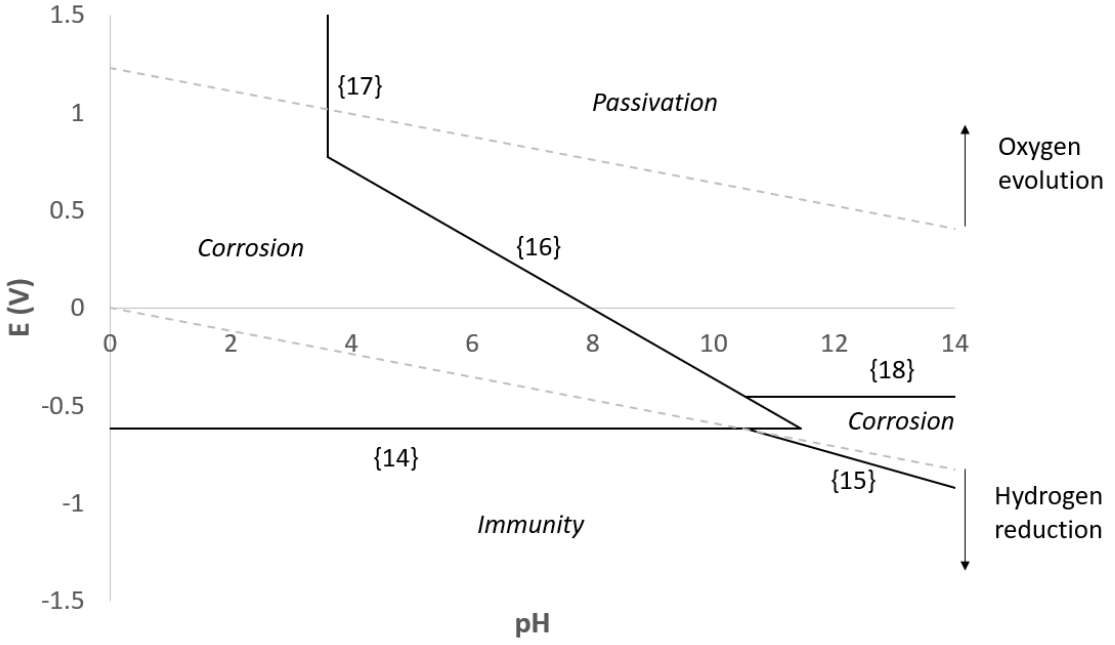

Figure 6: Pourbaix diagram of iron at 25°C

Various zones of corrosion, immunity and passivation can be noticed on the diagram of Fe-H_2O system. As pH decreases, the zone of corrosion increases. However, the actual rate of corrosion cannot be predicted from the diagram. Potential shifts to passive region in the neutral solution develops a protective layer on the metal surface. As noticed from the Pourbaix diagram, a potential shift to -0.8V would make metal immune from corrosion [20].

The corrosion rate of iron is affected by the cathodic reduction reaction. Whitman et al. studied the effect on the rate of corrosion in aerated water [8]. It is noted that for electrolyte of pH less than 4 (acidic solution), the rate of corrosion is higher as the H^+ ions are available for reduction and the oxide is soluble in aerated water. Additionally, dissolved oxygen is reduced cathodically to acid during this process. Steels with higher carbon content are observed to have a higher corrosion rate for lower pH. Carbon content increases the rate of reduction for H^+ ions and the cathodic reaction is under activation control. However, this is not the case for solutions with pH 4 to 10. Due to the uniform diffusion of dissolved oxygen, the rate of corrosion is nearly constant. Thus, the rate is controlled by the diffusion process. Solutions with higher pH (pH > 10), form a passive ferric oxide film on iron in the presence of dissolved oxygen. Hydrogen ions are involved in acid solution and as the pH increases, water molecules react directly with the metal (Figure 7) [7].

Hence, consideration of solution pH is vital for an effective protection system. The effect of solution pH is experimentally studied using a novel corrosion protection system. The results are presented in the following chapters.

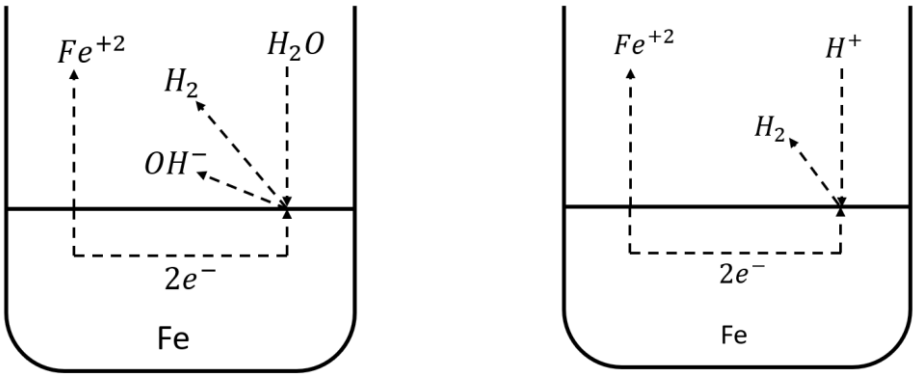

Figure 7: Uniform corrosion in (a) neutral or alkaline solution and; (b) in acidic solution

2.3.2. Effect of Temperature

In addition to solution pH, corrosion rate is also affected by the change in temperature. The rise in temperature, raises the rate of ion activity. Hence, elevated temperatures increase the rate of corrosion [20]. Further, a passive metal may become active at elevated temperatures.

As stated above the occurrence of an oxidation chemical reaction depends on ΔG. The Gibbs free energy of formation at constant pressure can be stated as shown in Equation 19 where ΔS° and ΔH° are entropy and enthalpy changes respectively. For constant entropy and enthalpy, changes in Gibbs free energy with respect to temperature is used to obtain the Ellingham diagram. It shows a linear metal-gas oxidizing behavior for changes in temperature (T) [11].

$$\Delta G^{\circ} = \Delta H^{\circ} - T \cdot \Delta S^{\circ} \tag{19}$$

Initially, the steel corrosion rate increases for heating above the room temperature [8]. However, dissolved oxygen solubility reduces at higher temperatures. Therefore, the corrosion rate decreases if the corrosion is happening in an open system at temperatures above 80°C. Unlike an open system, where oxygen escapes at higher temperature, closed systems can retain the dissolved oxygen. Thus, even above 80°C the rate of corrosion increases. Corrosion mechanism other than the uniform corrosion takes place above 50°C for steel [8]. Aeration cells may be formed at these high temperatures which leads to pitting or irregular corrosion.

The exponential dependence between corrosion rate and temperature is observed by Popova et al. [27]. Corrosion in acidic solution is governed by hydrogen depolarization. Hence, a decrease in hydrogen evolution overvoltage at high temperature is seen. The protective passive layer is less effective at high temperature as the ion diffusion through the passive film increases [28]. The passive layer is more inhomogeneous that supports the mobility of ions through it. Thus, several researchers have observed an increase in corrosion rate due to an increase in temperature [24] [29]. Additionally, an inverse relation is seen for corrosion potential and temperature [29]. Thus, the effect of temperature is observed by many investigators.

Despite numerous investigations to study the effect of solution temperature and pH, the singularity of these results does not add much value for risk management of the infrastructure. Though these results are vital, metal degradation is also affected by other factors. Corrosion in soil is a vital problem for the utility industry.

2.3.3. Corrosion in Soil

Degradation of metals in soil is considered to be a multi-step process due to the variation in the composition of the earth. Though, at the core of the corrosion in soil, is the electrochemical process at the surface of the metal [30]. At the metal and soil interface, local micro-environment that is affected by macro conditions (such as rain and temperature) control the process of corrosion [30]. The corrosion performance of ferrous metals in soil has been extensively studied in the past [30] [31] [32]. Researchers have considered the impact of parameters like humidity, temperature, pH, soil porosity and the influence of the external environment. Consideration of external environmental factors such as seasonal variation in temperature and rainfall is found to affect the localized environment at the metal interface [30]. Largely, researches related to metal exposed to soil environment can be categorized into: (1) laboratory-based experiments and (2) study of metals in the field (buried).

Weight loss measurements in solutions designed to mimic soil condition is done by Wu et al. [31]. The pH of these solutions is adjusted using sulphuric acid H_2SO_4 and the composition used to simulate soil condition is made of sodium chloride (NaCl), sodium sulfate (Na_2SO_4), magnesium sulfate ($MgSO_4$), calcium chloride ($CaCl_2$), sodium bicarbonate ($NaHCO_3$) and potassium nitrate (KNO_3). However, any reason for using the solution composition is not provided. The electrochemical tests on the steel sample indicated that parameters like corrosion current and potential (I_{corr} and E_{corr}), are pH dependent. Authors concluded that the highest mass loss and I_{corr} are observed for solution pH of 3. Similarly, electrochemical tests on steel sample in a solution composed of potassium chloride (KCl) is performed by Benmoussa et al. [32]. The solution composition used, mimics the soil in Algeria. As concluded by Wu et al., it is found that the temperature and acidity of the solution increases its aggressivity. The protective film on the metal surface is deposited over time and decreases the corrosion rate. The charge transfer resistance that affects the rate of corrosion is increased by the protective layer.

The effect of soil moisture content on the corrosion is investigated by Gupta et al. [33]. Soil samples are taken from three different sites in India and are used for the laboratory tests. To determine mass loss, metals exposed to soil for 180 days are used. Significant effect of moisture content on mass loss due to corrosion is seen. Additionally, a close correlation between mass loss and the moisture content is found. It is concluded that the mass loss increases up to an intermediate moisture content (about 65% water holding capacity) and reduces thereafter. Moreover, the lowest mass loss is logged in for high resistivity soils. Likewise, the correlation of corrosion current density with the moisture content is found by Murray et al. [34]. Indoor and outdoor experiments in different soils are carried out. It is concluded that the soil with the same moisture content has the same corrosion current density. The effect of rain on the soil moisture content and current density is clearly presented using the in-situ electrochemical impedance spectroscopy (EIS). The correlation of the soil resistivity and the moisture content is found, and the similar equivalent current density values were observed by Gupta et al. and Murray et al. Unlike Gupta et al., any intermediate point after which the mass loss decreases with increasing moisture content is not found by Murray et al., predominantly because the tests are carried out with soils of lower moisture content. On the other hand, the effect of soil along with the backfill material is studied by Norin et al. [35]. Generally, utility companies excavate to lay a grillage foundation or a pipe. The trench is backfilled with the material transported from elsewhere. Thus, the environment around the metal structure is heterogeneous mixture of various contents including the original soil. The high localized corrosion due to backfill material is studied by Norin et al. Unlike localized corrosion, uniform corrosion is seen to negatively correlate with the soil resistivity and is positively associated with the water content. Similar to Murray et al., any peak in the variation of uniform corrosion rate is not found by Norin et al. As a result, a strong correlation between soil moisture content and uniform corrosion rate is found by many researchers.

Soil moisture is the prime parameter that influences its resistivity [22] [36]. This is because the soil moisture content stimulates aeration and dissolution of mineral components. The oxygen transport by convection from the atmosphere to the steel surface is dependent on the moisture content. A detailed experimental study by Akkouche et al. shows the soil with 60-70% moisture saturation has the highest corrosion rate. For higher moisture content, the corrosion rate is lower as the soil pores are filled with an electrolyte

which hinders oxygen transportation. The critical moisture content behavior is also reported by Gupta et al.

Relevant hydrology literature indicates that saturation water content may vary for different soils. Water content for different soils as a function of sand content is found by Neale et al. [37]. It is seen from the results that the moisture content varies from 0.5% to 217%. A soil survey test standard is developed by American Water Works Association (AWWA) [38]. By assessing the soil characteristics for various factors mentioned in the standard, a point-based system can be used to determine the soil corrosivity. Several factors considered for soil-test evaluation are resistivity, pH, redox potential, sulfides and moisture. Thus, these factors should be considered as the corrosion rate is affected by soil and other conditions.

The overview of factors that affect the degradation process is presented by Cole et al. [30]. The influence of macro-environment features that include (but are not limited to) rainfall, temperature and other climatic and terrain factors is given. The effect of these factors is relevant. Thus, a multiscale model for soil corrosion is proposed. These factors are shown in Figure 8. However, the model encompasses factors only of first-order of importance to oxygen, solute concentration and moisture in the soil. A thorough literature review is done by Cole et al. to conclude that the effects of soil moisture content is paramount.

Moreover, the corrosion current density is affected by temperature. At ambient or lower temperature, the cathodic potential of 0.85V is sufficient to protect the target metal. However, at elevated temperatures this does not provide enough protection as observed by Kim et al. [39]. Hence, a more negative potential is required for sufficient protection at elevated temperatures. Cathodic potential of 1.35V is required to sufficiently protect steel at 80°C [25].

Furthermore, Sancy et al. found the effects of oxide film development on the metal surface to be very high [40]. Researchers compared the corrosion rate of the outer surface of the pipe in water and sand. Corrosion was found by an order of magnitude higher in sand. The restrictive factor that controls the corrosion rate is the diffusion of oxygen. The porous oxide layer built on the metal surface decreases the electrochemical current with time. When target metal is immersed in sand, the diffusion needs to occur through both

sand and porous oxide layer. This makes the process slower as compared to corrosion in water. Corrosion is regarded as a complex process as there are many other variables affecting the process. Bushman et al. combined the effects of various factors to develop a multiple regression model to predict the corrosion rate [41]. The failure time due to corrosion can be found by using Equation 20, where Y is the mean time for corrosion failure, B_k is the constant, e is the error factor for normal probability distribution and X_k is each independent variable that affects corrosion.

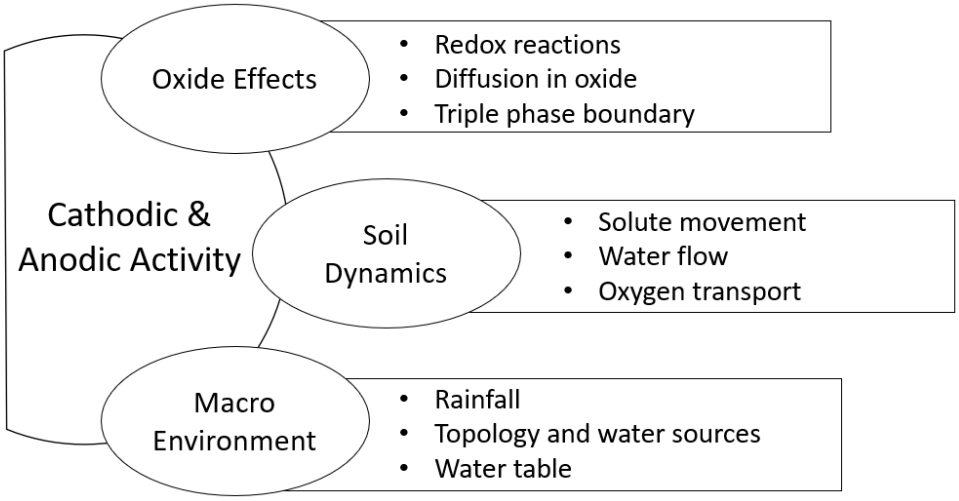

Figure 8: Multi-scale model for corrosion in soil

$$Y = B_0 + B_1X_1 + B_2X_2 + \ldots + B_kX_k + e \quad (20)$$

Due to many factors that affect corrosion in soil, uncertainty may arise for such models that predict corrosion. Ferreira et al. designed an experiment to simulate soil conditions/chemistry to compare results obtained from the field tests [42]. It was concluded that the soil resistivity varied for in-field tests and laboratory-based simulation experiments. Thus, various literature also emphasizes the difficulty in comparing corrosion results obtained from different test sites.

2.4. Proof-of-Concept

It is difficult to address the non-uniform corrosion of metal structure. Thus, changing environmental conditions should be considered for a system to be effective. Additionally, it is important to control the protection parameters to avoid over-protection or under-protection [43]. Mendoza et al. used the standard cathodic protection potential (-0.85V) to protect steel buried in the soil [44]. The laboratory experiments show that the cathodic protection potential under-protects the target metal in acidic soils. An effective system should update the protection parameters regularly by measuring the corrosion behavior of the target metal. The undesired potential throughout the structure caused by over-protection leads to an acceleration of the corrosion process [45]. Therefore, monitoring the corrosion status and updating the corrosion parameters regularly is necessary for reliable protection. Generally, measurement cost for effective protection is paramount in the utility industry. On-site testing must be conducted by a protection system to be effective.

To address these limitations, Patel et al. proposed a proof-of-concept of an Adaptive Corrosion Protection System (ACPS) [14]. From various cathodic protection criteria, it is claimed that the E-log-I criterion is more accurate and scientifically fundamental [21]. E-log-I criterion allows onsite testing that takes into consideration the interaction of target metal with its environment. The ACPS test procedure is shown in Figure 9. An Open Circuit Potential (OCP) of the electrochemical cell is obtained. Thereafter, polarization curve is obtained by sweeping the potential. Protection parameters are systematically extracted and the protection current is controlled and appropriate potential is supplied to the target metal. The extracted optimum protection parameters reflect the changing environment conditions. The ACPS works in a feedback loop that monitors the corrosion status by electrochemical measurements at a defined interval. The proof-of-concept presented earlier is used for this research.

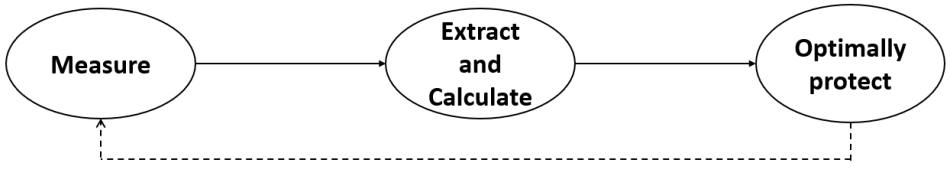

Figure 9: Adaptive Corrosion Protection System test procedure

Chapter 3.

Objectives

The idea about an adaptive system for effective corrosion protection system is used for this research. To support and verify the proof of concept, Patel et al. carried out laboratory based systematic experiments. Using potentiostat (PARSTAT 4000 from Princeton Applied Research) operated using a personal computer, an initial validation was performed. A Tafel Plot was obtained to manually extract protection parameters. Thereafter, secondary system was initialised with automatic feedback-loop based capability. This was done using a simple DC source meter (Keithley Model 2400) integrated with a personal computer. The concept of an adaptive corrosion protection system was supported by effective experimentation results.

This research is part of an ongoing project at Simon Fraser University in collaboration with BC Hydro and Powertech Labs. The motivation for this work is to develop a miniature, standalone system for in-field installation. The ACPS project plan is shown in Figure 10. Thus, optimizing and establishing ACPS algorithm for modular standalone device is required. A large and expensive setup consisting of either potentiostat or DC source meter cannot be installed for in-field implementation. Using the proof-of-concept presented earlier, a technically feasible and financially viable standalone system solution is required. Hence, an effective system design is carried out.

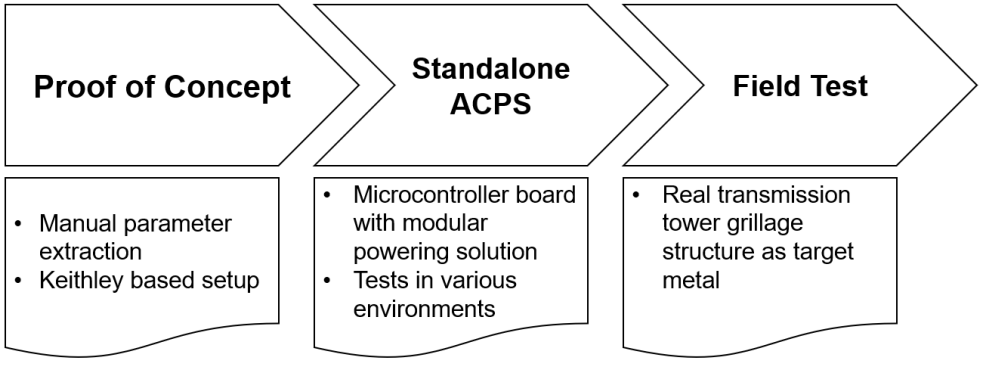

Figure 10: Adaptive Corrosion Protection System project overview

The goal of this work is to develop a comprehensive understanding of the corrosion behavior of steel in different environments using the novel Adaptive Corrosion Protection System (ACPS). Using the proof-of-concept proposed earlier, this work aims to design a new standalone system that can be used for the field test. A new standalone ACPS hardware and software module is designed that works using the grid power and off-grid solar energy. This dissertation primarily focuses on the electrochemical aspect of the industrial research project. The main objectives are: (1) to design a standalone adaptive corrosion protection system; (2) to design modular powering solution; and (3) to validate standalone ACPS performance in various environmental conditions.

Key Technical Objectives:

1. Design a stand-alone Adaptive Corrosion Protection System (ACPS)
    a. Develop ACPS algorithm for modular standalone solution based on the proof-of-concept presented by Patel et al. [14]
    b. Design ACPS based corrosion protection solution for transmission tower grillage structures
        i. Identify validation criteria in coordination with BC Hydro and Powertech Labs
2. Design modular powering of ACPS for grid-powered and off-grid system
    a. Integrate wide range of power capabilities
    b. Test the powering solution for standalone system
3. Validate standalone ACPS performance in various environmental conditions
    a. Measure protection efficiency using the new feedback loop based cathodic protection system
    b. Compare the corrosion protection efficiency of the novel corrosion protection system with the NACE standard Impressed Current Cathodic Protection (ICCP) system

c. Assess the impact of environmental factors on the corrosion protection techniques

In practice, this work will also contribute towards the ongoing project to develop a smart-grid based corrosion protection system. Thus, a stand-alone test set up is required for in-field test. The following phase of the research project will require scaling-up the test model. The project work requires an ongoing collaboration with industry partners to learn system and application requirements. A better understanding of the factors that lead to corrosion, coupled with information and alterations related to the novel adaptive corrosion protection system can aid the developments of the ongoing research project.

Chapter 4.

Preliminary Analysis

The Adaptive Corrosion Protection System measures the electrochemical response of the target metal in a corrosive environment to obtain Tafel plot and extract protection parameters. Typically, E_{corr} and I_{corr} values are used to calculate the corrosion rate or the penetration rate of the target metal. Therefore, a simple LabView and Keithley (DC Source meter) based ACPS mechanism is prepared for automating preliminary analysis.

Unlike the potential based ICCP system, the ACPS avoids over-protection or under-protection of the target metal [14]. The feedback loop measures the analytical electrochemical behavior to optimize system performance according to the dynamic environment changes. A comparative analysis is carried out in the laboratory environment. The comparison is conducted using saline solution at different temperatures. The effectiveness of the ACPS along with the ICCP standard method is tested by measuring weight-loss of the target metal.

4.1. Experimental Set-up

The systematic study to validate and compare the ACPS system with the NACE standard method (ICCP) is carried out in the lab environment [19]. The experimental setup is prepared using 3% NaCl solution as the corrosive medium and an ASTM A36 (UNS K02600) hot rolled steel sample as the target metal. A36 is the most commonly used mild steel. It is used in the construction of bridges, oil rigs, buildings etc. [46]. The chemical composition of A36 steel is shown in Table 2. Two different target metal samples are prepared to compare the performance of the proposed adaptive system and the ICCP system. A third metal sample is prepared and is allowed to corrode freely. Same surface area (2.5 cm x 2.5 cm x 0.5 cm) of the target metal coupons is selected to ensure consistency between different methods. Before starting the experiment, the metal samples are thoroughly cleaned using isopropyl alcohol (IPA) and oven-dried to evaporate moisture from the metal surface. The weight of all three metal coupons is measured before and after the experiment to determine the weight-loss. Three glass beakers are prepared with

the same electrode setup. The volume of the corrosive medium (400 ml, 3% NaCl solution) for each beaker set-up is consistently same for all the experiments.

Table 2: Chemical composition of ASTM A36 steel

Element	Carbon (C)	Copper (Cu)	Iron (Fe)	Manganese (Mn)	Phosphorous (P)	Silicon (Si)
Content	0.25-0.29%	0.20%	98.00%	1.03%	0.04%	0.28%

Adaptive Corrosion Protection System

For the adaptive corrosion protection system (ACPS), the three-electrode set-up is prepared, and the Britton curve is obtained by sweeping the potential on the target metal (working electrode) with respect to the reference electrode. The standard calomel electrode (SCE) is used as the reference electrode and an inert graphite bar is used as the counter electrode. The potential sweep starting from the anodic region to the cathodic region is selected to obtain the polarization curve. The corrosion current (I_{corr}) and the corrosion potential (E_{corr}) are extracted from the polarization curve. The extracted protection parameters are supplied to protect the target metal. During experiments, the protection parameters are extracted every hour by re-measuring the Tafel segment of the polarization curve. A LabView based automated system is prepared to avoid human interaction.

Impressed Current Cathodic Protection System

Similar to the ACPS, the three-electrode configuration is established for implementing the ICCP system. The standard calomel reference electrode and the inert graphite bar as the counter electrode are used. The open-circuit potential is measured in the beginning and the source potential for the protection mode is calculated by adding -0.770V. This potential is applied with respect to the SCE to protect the target metal.

Unprotected System

For the freely corroding metal sample, the metal coupon is suspended into the beaker and allowed to corrode freely for the entire test duration.

The experimental setup is shown in Figure 11. After each experiment, the target metal coupons are sonicated for 30 minutes in IPA to ensure all loose particles are removed from the metal surface. Subsequently, the metal coupons are oven-dried to evaporate the moisture content. The metal coupons are then weighed to compare the loss of weight after the tests. Same experiments are performed at different temperatures (30ºC to 80ºC) in 3% NaCl solution. Each experiment is conducted for 24 hours and both protected and unprotected specimens are tested simultaneously. The weight loss (*W*) for all three samples is analyzed to calculate the protection efficiency of the system. The protection efficiency (ε) of the system is calculated using Equation 21:

$$\varepsilon(\%) = \frac{W_{unprotected} - W_{protected}}{W_{unprotected}} \times 100 \qquad (21)$$

where, ε is protection efficiency

$W_{unprotected}$ is weight-loss of unprotected sample

$W_{protected}$ is weight-loss of protected sample

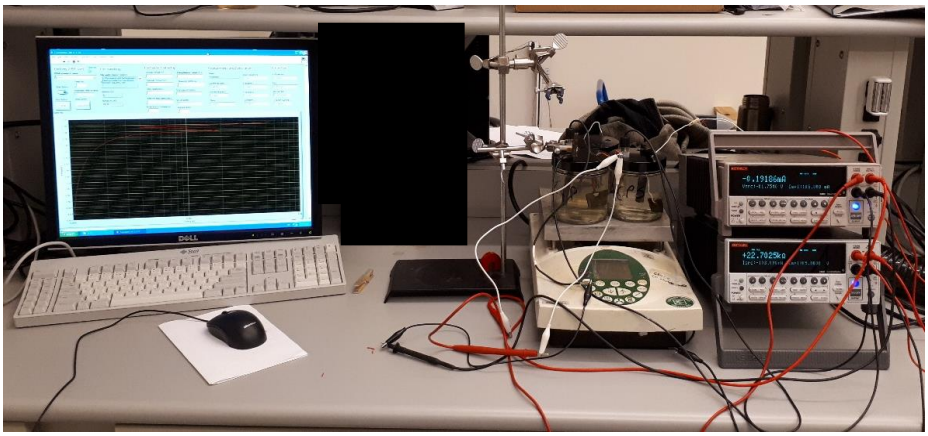

Figure 11: Electrochemical test setup for preliminary analysis

4.2. Results and Discussion

This section presents the results of the preliminary experimental tests performed on the three test setups discussed above. The weight-loss after 24 hours for all three setups at different temperatures is shown in Figure 12. As mentioned earlier, the tests are performed in the highly corrosive environment (3% NaCl solution) to accelerate the corrosion effect on the metal coupons.

During the first experiment at 30°C (Figure 12(a)), the unprotected sample, the ACPS protected sample and the ICCP protected sample realized 12 mg, 1 mg, and 3 mg weight-loss respectively. This weight-loss results in 92% and 75% protection efficiency of the ACPS and the ICCP systems respectively. A similar trend is observed for the other temperature settings. The protection efficiency of the test setups at different temperatures for different test setups is calculated, tabulated (Table 3) and plotted (Figure 13) to briefly summarize all the results. These results clearly indicate that the adaptive feedback loop of the novel current sourced corrosion protection system offers comparable corrosion protection behavior as the NACE standard ICCP system.

In the adaptive system where the protection current is extracted from the Tafel segment, a minor deviation in extraction may result in the failure of the system. However, the ACPS system quickly adjusts to any changes and protects the samples effectively as repetitive measurements are taken.

From the data analysis, it is important to notice that the ACPS based corrosion protection system suffers the protection efficiency as the test temperature increases. On the contrary, the protection efficiency for the ICCP based system improves as the temperature increases. At ~60°C, the protection efficiencies of the ACPS based system and the ICCP based system is in close proximity.

It is also worth noting that the data accuracy and resolution can be improved by using a more accurate and sensitive weighing scale. Additionally, accurate corrosion rate and hence the protection efficiency of the protection systems can be derived directly using the electrochemical behavior in the future. Long-term tests can be performed to validate the adaptive mechanism and compare it with the ICCP system.

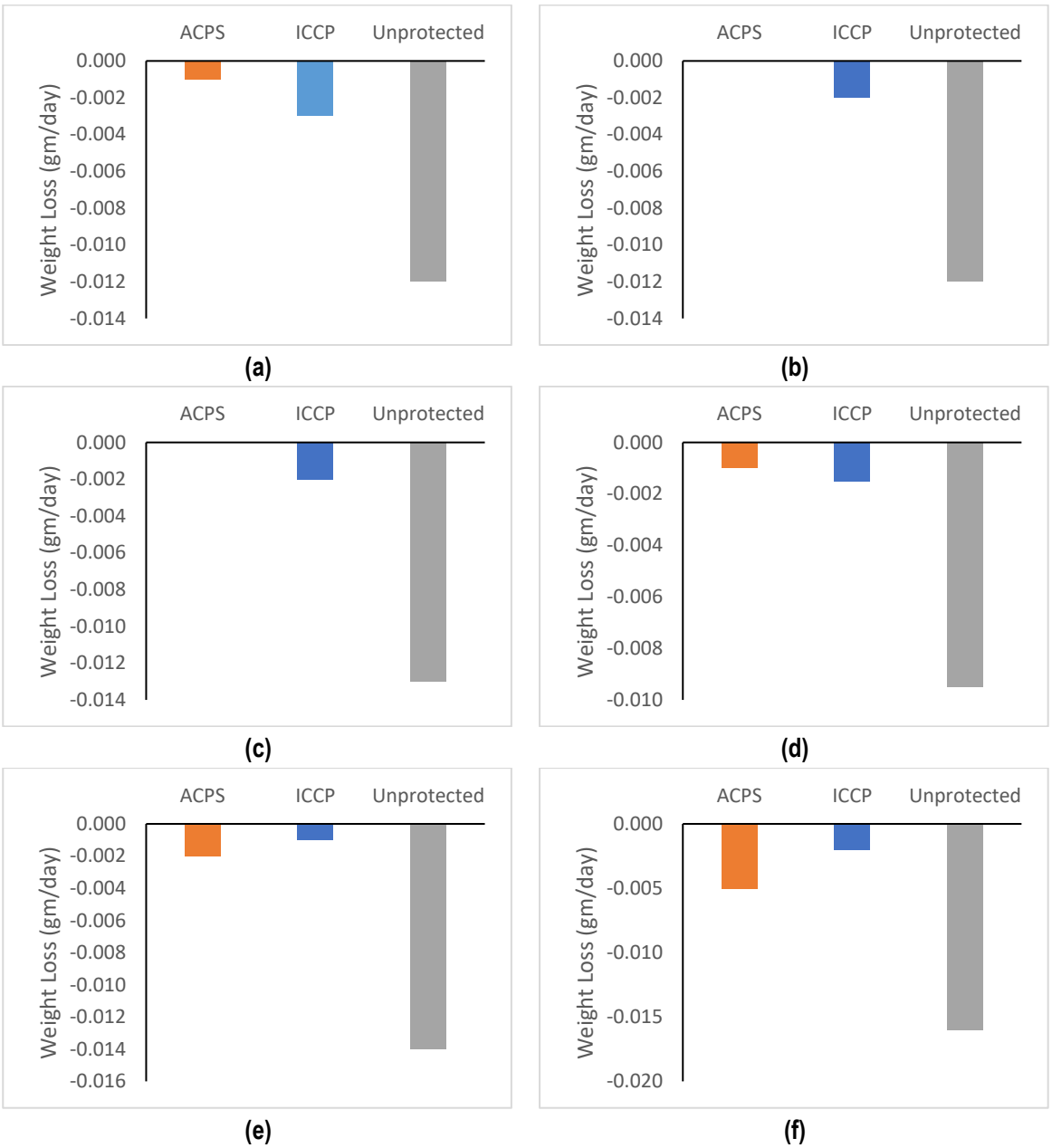

Figure 12: Weight loss comparison of ACPS protected metal, the ICCP protected metal and the unprotected metal sample at (a) 30°C; (b) 40°C; (c) 50°C; (d) 60°C; (e) 70°C; (f) 80°C

Table 3: Protection efficiency at different temperatures

Protection Efficiency	Temperature (°C)					
	30°C	40°C	50°C	60°C	70°C	80°C
ACPS	92%	100%	100%	89%	86%	69%
ICCP	75%	83%	85%	84%	93%	87%

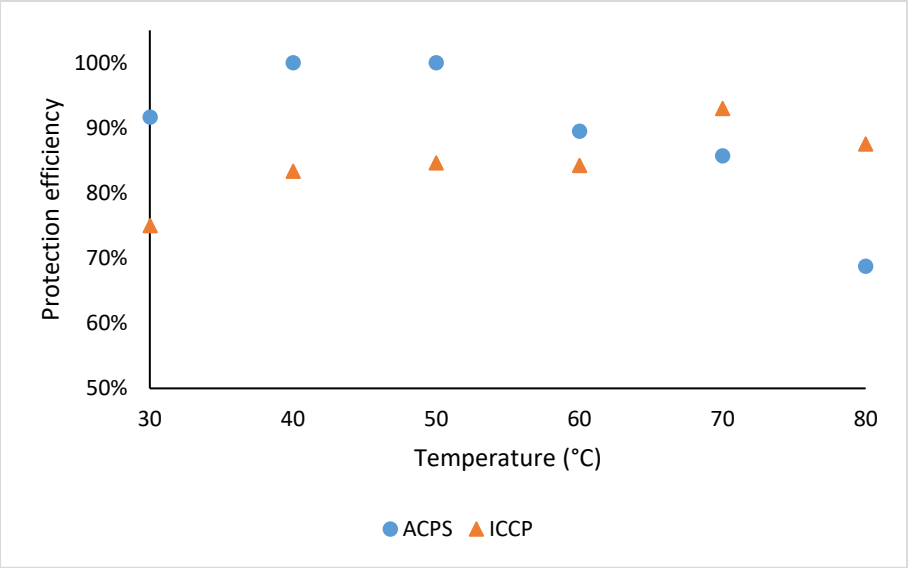

Figure 13: Protection efficiency comparison of ACPS and ICCP protected metal

Chapter 5.

Corrosion Protection Using a Standalone ACPS Solution in Different Corrosive Environments

Following the preliminary analysis, a stand-alone ACPS system module is developed. The modular system is designed that works using off-grid solar energy. Using the novel ACPS micro-controller board and booster unit for wide range power capabilities, a systematic experimental study is performed in the lab environment. The modular ACPS is used to protect the target metal in various corrosive mediums at different temperatures and pH. The results are compared with the NACE standard ICCP system.

5.1. Materials and Methods

As described in the previous chapter, experiments are performed in the lab using ASTM A36 steel sample as the target metal. An inert graphite rod (Walfront, China: part#80ick5o1gm) is used as the counter electrode and a standard calomel electrode (SCE) (Koslow Scientific Testing Instruments, NJ, USA: part#1001) is used as the reference electrode for all the experiments.

Adaptive Corrosion Protection System

As described in detail in previous sections, an ACPS electrochemical test setup is used to obtain the Britton Curve by sweeping potential on the working electrode (target metal) with respect to the reference electrode (standard calomel). The polarization curve is obtained using anodic to cathodic sweep and the protection parameters are extracted. The protection power based on the extracted parameters is supplied to protect the target metal. The test procedure of the ACPS is shown in Figure 14. The measurement cycle is repeated every 60 minutes and the protection parameters are updated automatically.

An independent ACPS system solution is designed. Interface, hardware and firmware are specifically developed for this project. This makes the system portable, modular and low-cost to make it suitable for variety of applications. Modular powering solution is designed for a standalone system. This novel standalone ACPS can be used

with grid-power and off-grid solar energy. Hence, ACPS can be deployed for infrastructure monitoring and protection even at remote locations where grid power is unavailable.

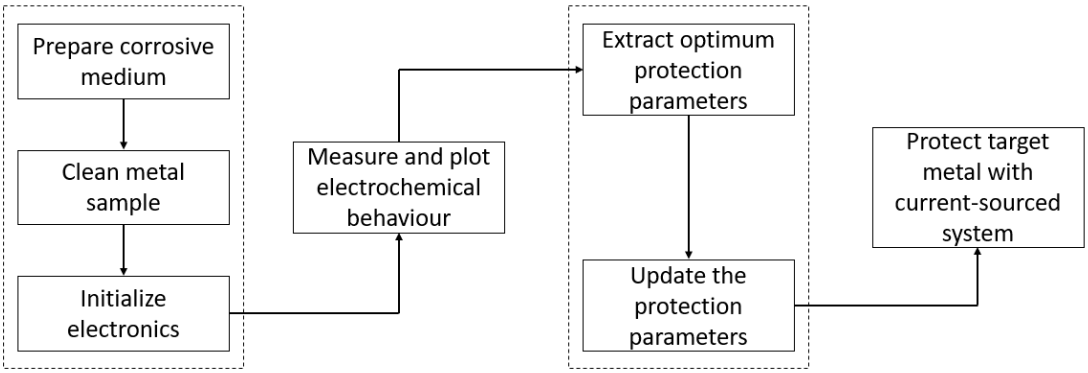

Figure 14: Experimental procedure of the Adaptive Corrosion Protection System

Standalone ACPS solution is used for a systematic electrochemical experimentation. Instead of using grid power, the novel ACPS is used using off-grid solar energy (Figure 15). The system uses ACPS microcontroller board in integration with the Raspberry Pi [47]. The ACPS interface runs on the Raspberry Pi 3 (Model B+). Raspberry Pi is a small, portable and low-cost computer that powers the ACPS microcontroller board and also allows effective data transfer and storage. The ACPS microcontroller board is a custom design board that uses ATxmega256A3U microcontroller. The microcontroller board is capable of ±1.5V and 15mA. The ACPS interface along with its workflow and microcontroller board are shown in the appendix.

The ACPS algorithm works in an adaptive feedback loop consisting of several steps. As the program is executed, it measures the Open Circuit Potential (OCP) of the electrochemical cell (Step-1). Electrochemical response is obtained in the form of a polarisation curve with the Tafel segment for the user-defined potential interval. Protection parameters are automatically extracted (Step-2). Thereafter, the rate of change of potential is measured at constant current (protection parameter). This chronopotentiometry experiment is continued for user-defined duration (Step-3). Step-1 commences after the end of Step-3. These experiments are executed in a loop until user-stops the program. After step-2 and 3, data file (.csv) and image file (.png) are saved automatically.

One of the integral parts of the system is its booster unit. Corrosion of any target metal depends on its surface area. Thus, corrosion protection parameters are surface area dependent. Booster unit is designed solely to integrate wide range of power capabilities. The booster unit is capable of ±24V and 3-5A. Experiments using small metal coupons (as is the case here) can be performed without the booster unit if using grid-power. However, booster unit is used to check its effective integration and to use off-grid solar energy. A 100W monocrystalline solar panel is used for this work. The ACPS system solution is shown in Figure 16

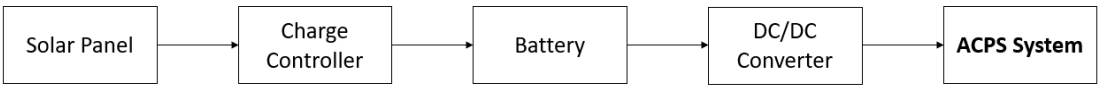

Figure 15: Off-grid solar power based Adaptive Corrosion Protection System

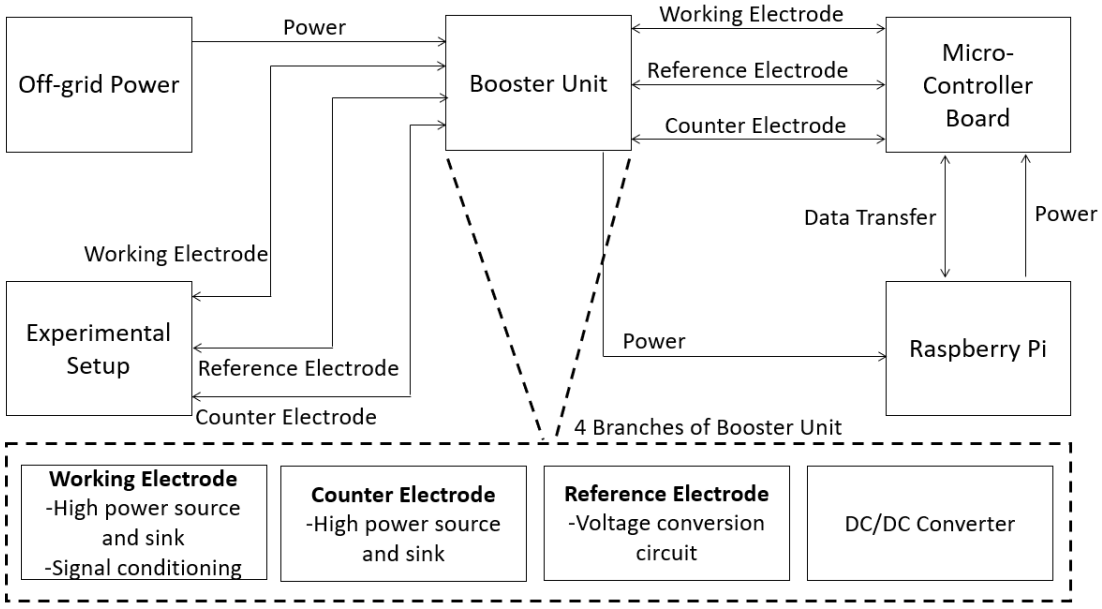

Figure 16: Portable, modular, standalone Adaptive Corrosion Protection System solution

Impressed Current Cathodic Protection System

The electrochemical set-up of the ICCP based protection system is also designed using an inert graphite rod as the counter electrode and a standard calomel electrode as the reference electrode. The source potential for the protection mode is calculated using the open circuit potential (adding -0.770V to the open circuit potential (OCP) as per the NACE standard). The source potential is applied with respect to the SCE.

Unprotected System

The target metal is suspended into the corrosive medium for the entire test duration and is allowed to corrode freely.

5.1.1. Experimental Set-Up for Corrosive Medium at Different Temperatures

The experimental setup is prepared using 3% saline (NaCl) solution as the corrosive medium for three metal (A36 steel) coupons. One metal coupon for each of the ACPS protected setup, the ICCP protected setup and the freely corroding setup is used to calculate the protection efficiency. The metal coupons of the same surface area (2.5cm x 2.5cm x 0.5cm) are selected to ensure consistency between different methods. Before each experiment, the metal coupons are thoroughly cleaned using isopropyl alcohol (IPA) and oven-dried to evaporate moisture from the metal surface. A glass beaker with 400ml of 3% NaCl solution at the selected temperature is used as the corrosive medium.

The temperature of the saline solution is varied from 30°C to 80°C with 5°C step. Simultaneously all three setups are tested for 120 hours. After each experiment, loose debris on the target metal coupons is removed by ultra-sonication (TruSonik TS-2.5L Ultrasonic Cleaner) for 50 minutes in IPA followed by an oven-drying step to evaporate the moisture content. Subsequently, weight loss measurements are done at the end of each experiment to compare the three systems. The average weight loss per 24-hours is calculated and the data is represented in the subsequent sections.

5.1.2. Experimental Set-Up for Corrosive Medium of Different pH

The corrosive medium of different pH (from pH 2 to pH 12) is prepared using 1N of HCl and 1N NaOH by titration. Similarly, as described above, three A36 target metal samples are used to compare the performance of the ACPS system, the ICCP system, and the unprotected system. The metal coupons of same surface area (2.5cm x 2.5cm x 0.5cm) are used. Before starting the experiment, the coupons are thoroughly cleaned using IPA and oven-dried. Each setup uses 400ml of the specific pH solution as the corrosive medium. All experiments are performed for 120 hours. After each experiment, the coupons are sonicated for 50 minutes in IPA. Subsequently, the metal coupons are oven-dried, and the weight loss measurements are performed.

The experimental set-up is shown in Figure 17. Similar to the preliminary analysis, weight loss for all metal coupons are analyzed to calculate the protection efficiency.

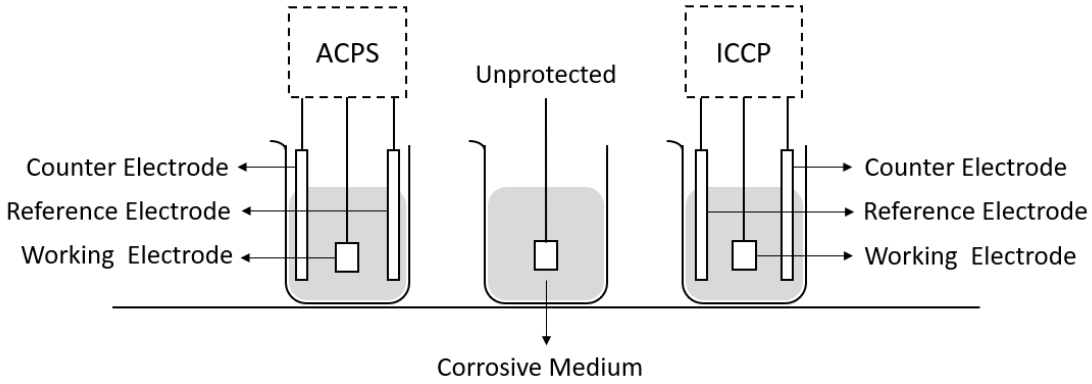

Figure 17: Experimental setup of a comparative analysis

5.2. Results and Discussion

Metal corrosion depends on the interaction of the metal coupon with various corrosive mediums. This section presents the outcome of the laboratory experiments. The results for the temperature and pH experiments are given below. The protection efficiency comparison of the adaptive system and the standard ICCP system is discussed in its individual sections.

5.2.1. ACPS Performance at Different Temperatures

As mentioned earlier, the tests are performed in the aggressive environment (3% NaCl solution) to accelerate the corrosion effect on metal coupons. The average weight-loss per 24 hours for all three setups at different temperatures is shown in Figure 18 and the data is given in Table 4.

During the first experiment at 30°C, the ACPS protected sample, the ICCP protected sample and the unprotected sample realized 0.85mg/day, 0.80mg/day and 4.80mg/day weight loss respectively. The weight loss results in 82% and 83% protection efficiency of the ACPS and the ICCP systems respectively (Figure 19 and Table 5). Cathodic protection is considered effective when the general corrosion rate is less than 25µm/year [21]. The corrosion rate at 30°C for the ACPS and the ICCP systems are 22.58 µm/year and 21.26µm/year respectively. A similar trend is observed for other temperature settings. These results clearly indicate that the adaptive mechanism for the current sourced corrosion protection system offers comparable corrosion protection behavior as the NACE standard ICCP system.

The rate of the activity of ions increases with an increase in temperature - this escalates the corrosion rate [20]. These results can be seen in Figure 18. Relation of corrosion rate with temperature is represented using Arrhenius equation (Equation 22) [48] [49] [50]. It can be noticed from the equation that the corrosion rate (i_c), increases exponentially with an increase in temperature (T).

$$i_c = Ae^{-\frac{E}{RT}} \tag{22}$$

Where, i_c is the corrosion rate

A is the Arrhenius factor

R is the universal gas constant

T is the absolute temperature

E is the activation energy

The diffusion rate of the electrolytes increases due to a rise in activation energy at higher temperatures. This increases the flow/transport of electrolytes across the metal surface, which raises the corrosion rate [49]. Kairi et al. indicate that dissolution of mild steel predominates on the surface at higher temperatures [51]. This increases the surface

kinetic energy, which accelerates the corrosion process. Malik et al. carried out experiments using 316L steel in corrosive mediums at different temperature (30°C to 80°C) and found that the corrosion rate is highest at 80°C and lowest at 30°C [52]. Additionally, Phelps et al. have suggested that the corrosion rate of the steel samples increases with increase in temperature [53]. Based on weight loss measurements it was concluded that the corrosion behavior of certain types of austenitic steels in sulfuric acid could be represented as active-passive regions. As discussed by Truman et al. the effects of chloride content and temperature are interrelated [54].

From the data analysis, it is noticed that the ACPS based corrosion protection system is an effective mechanism that provides comparable result as the standard ICCP method for the selected temperature range.

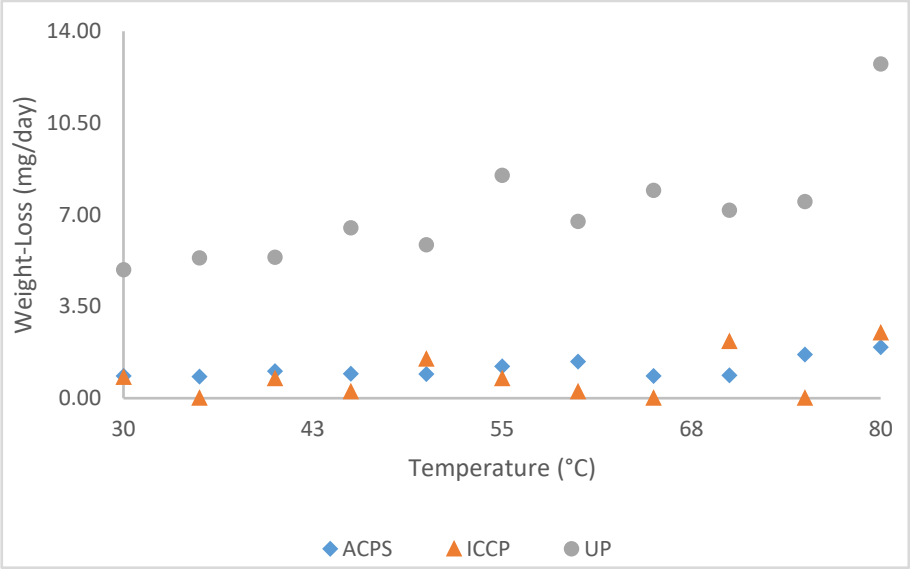

Figure 18: Weight loss for selected temperature range

Table 4: Weight loss at different temperatures

Weight-Loss	Temperature (°C)										
(mg/day)	30	35	40	45	50	55	60	65	70	75	80
ACPS	0.85	0.82	1.03	0.93	0.93	1.21	1.40	0.85	0.87	1.67	1.95
ICCP	0.80	0.00	0.75	0.25	1.50	0.75	0.25	0.00	2.17	0.00	2.50
Unprotected	4.90	5.35	5.38	6.50	5.85	8.50	6.75	7.93	7.17	7.50	12.75

Table 5: Protection efficiency at different temperatures

Protection Efficiency	Temperature (°C)										
(%)	30	35	40	45	50	55	60	65	70	75	80
ACPS	83	85	81	86	84	86	79	89	88	78	85
ICCP	84	100	86	96	74	91	96	100	70	100	80

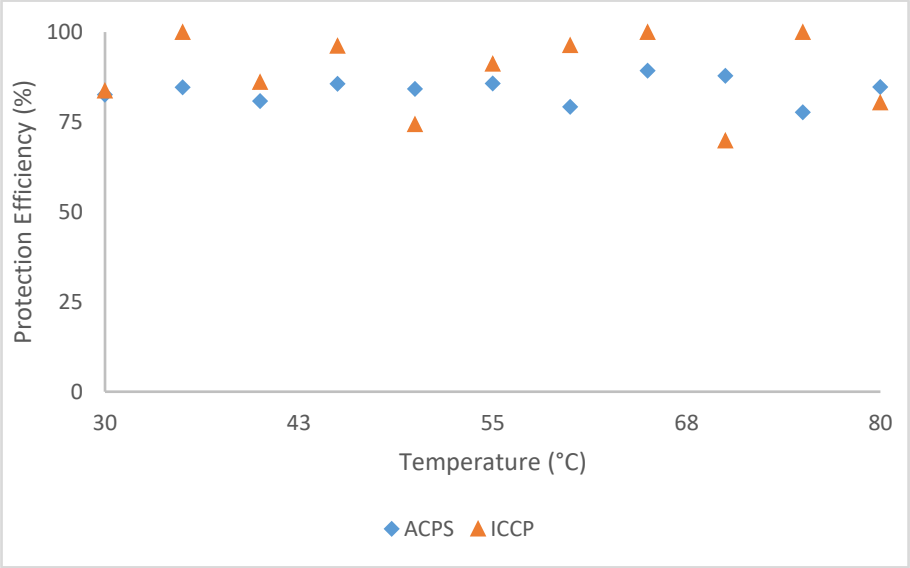

Figure 19: Protection efficiency of ACPS and ICCP for selected temperature range

5.2.2. ACPS Performance with Corrosive Medium of Different pH

As described earlier, a test facility was developed to examine and compare the results of two cathodic protection mechanisms. Corrosion with respect to the pH of the solution can be determined using Pourbaix diagrams [20]. Pourbaix diagrams are temperature dependent and represent the thermodynamic possibilities [55]. Therefore, all experiments were done at room temperature to maintain constant reaction kinetics. The results for these experiments are described in this section.

During the first experiment at pH=2 (Figure 20 and Table 6), the ACPS protected sample, the ICCP protected sample and the freely corroding sample realized 5.97mg/day, 5.75mg/day and 11.25mg/day weight-loss respectively. This weight-loss results in 47% and 49% protection efficiency (Figure 21) of the ACPS and ICCP systems respectively. With a decrease in the acidity of the corrosive medium, corrosion rate also decreases. The protection efficiency is calculated for different pH setups and plotted (Figure 21 and Table 7) to summarize the results. It is important to notice that the protection efficiency increases for both protective systems with a decrease in the acidity of the corrosive medium. Protection efficiency for both systems is in close proximity for all the pH values. However, weight-loss for the pH values higher than 9 fluctuates within ± 2 mg.

Hydrogen ions raise the redox potential of the aqueous solution which accelerates the corrosion process [49]. Malik et al. and Muslim et al. found that the corrosion rate generally decreases with increasing pH [49] [52]. Trivedi et al. present the relation (Equation 18) between pH and corrosion current from the studies conducted by various researchers [48]. The value of constant 'A' (Equation 23) differs for researchers in the range of 0.5 to 1.2 [48].

$$Log(i_c) = -A \cdot pH + B \tag{23}$$

where, i_c is the corrosion rate

A is a constant

pH is the solution pH

B is a constant

Thus, it can be concluded that the ACPS based system can provide similar protection efficiency as the ICCP method. It is worth noting that the data accuracy and resolution can be improved by using a sensitive weighing scale.

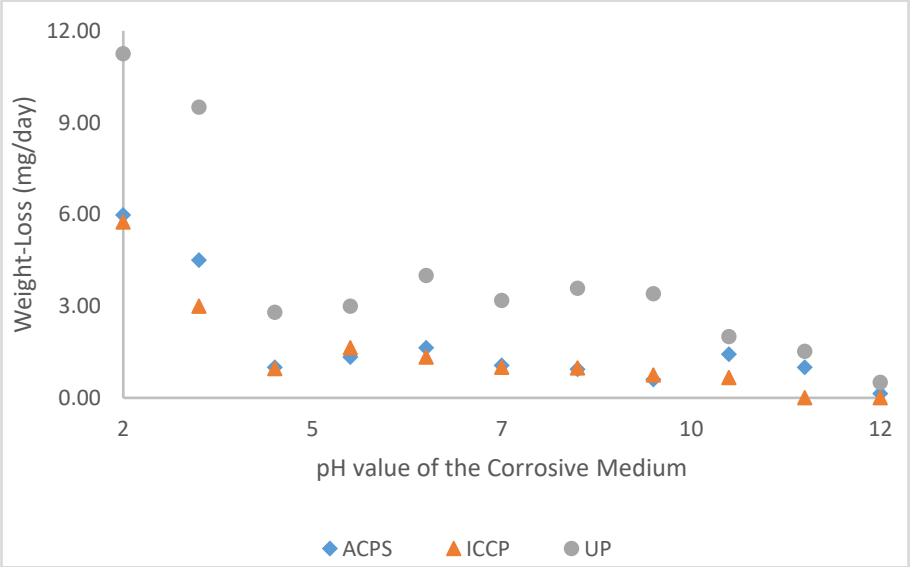

Figure 20: Weight loss for selected temperature range

Table 6: Weight loss at different solution pH

Weight-Loss	**Solution pH**										
(mg/day)	2	3	4	5	6	7	8	9	10	11	12
ACPS	5.97	4.50	1.00	1.33	1.63	1.06	0.94	0.60	1.42	1.00	0.14
ICCP	5.75	3.00	0.95	1.63	1.33	1.00	0.97	0.75	0.67	0.00	0.00
Unprotected	11.25	9.50	2.80	3.00	4.00	3.18	3.58	3.40	2.00	1.52	0.50

Table 7: Protection efficiency at different solution pH

Protection Efficiency	Solution pH										
(%)	2	3	4	5	6	7	8	9	10	11	12
ACPS	47	53	64	56	59	67	74	82	29	34	72
ICCP	49	68	66	46	67	69	73	78	67	100	100

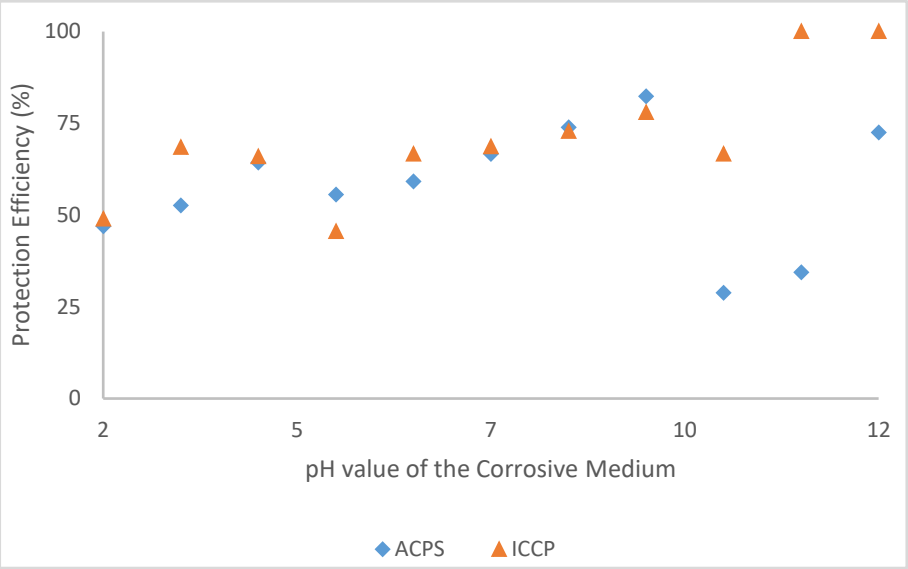

Figure 21: Protection efficiency of ACPS and ICCP for selected pH range

Chapter 6.

Validation in Soil Environment

Steel structures submerged in soil generally have a useful life of 5 – 10 decades [20]. However, environmental factors control the rate of corrosion. Thus, ferrous metal corrosion is a vital problem for the utility industry. A miniature grillage structure is submerged in soil and protected by ACPS based system integrated with off-grid solar energy. The experiment is done in an uncontrolled environment and the weather data available online by the Government of Canada is correlated with the ACPS performance. As outlined by various researchers, the soil moisture content has the utmost effect on the intensity of the corrosion [30] [33]. Factors of macro-environment, precipitation and temperature that directly affects the soil content are obtained by the weather station located at the Simon Fraser University (Burnaby). Unlike previous chapters, this chapter describes a long-term experiment in an uncontrolled environment.

6.1. Materials and Methods

A systematic long-term experimental study is performed using the miniature grillage structure of ASTM A36 steel. The ACPS based system is used to protect the structure submerged in soil. Efforts are made to effectively mimic the real soil environment. A tote (30in x 20in x 20in) (136.3L) is prepared for effective self-watering. Plastic pipes are kept at the base of the tote to retain water and maintain the soil moisture content (Figure 22). To allow extra water to flow out, an outlet is created at the base of the tote.

To construct a grillage structure that fits in the tote, angles, and channels of A36 steel is used. Dimensions and quantity of the grillage components are given in Table 8. Additionally, grillage components are joined together using 34 bolts, nuts and washers. The miniature grillage structure is shown in Figure 24. The tote is partially filled with garden soil to create a base for the grillage. The grillage is placed inside along with the $Cu/CuSO_4$ (Borin Manufacturing Inc. Stelth 2 SRE-007-CUY) reference electrode and graphite rod as the counter electrode (Figure 22). After three electrodes are stable and upright in their respective position, more soil is added in the tote. A total of 19.3kg garden soil is added into the tote to make sure all three electrodes are completely immersed in the soil. The

experimental setup for validation in soil environment using miniature grillage structure is shown in Figure 23. The tote is placed on the cart and the cart is placed in the patio outside the laboratory (Figure 24).

(a) (b)

Figure 22: (a) Plastic pipes at the base of the tote for self-watering and; (b) electrode placement in the tote

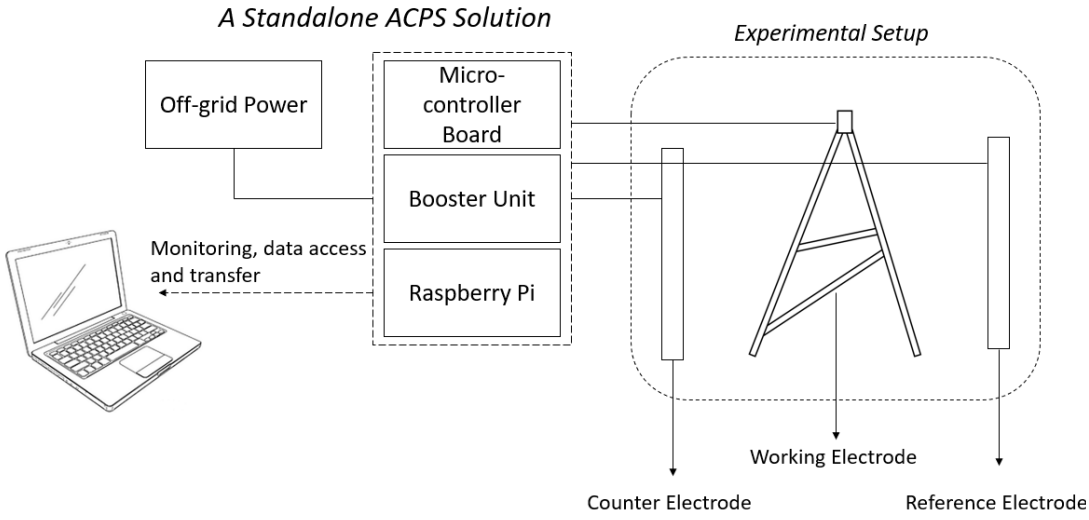

Figure 23: Experimental setup for validation in soil environment using miniature grillage structure

Table 8: Components used to make the grillage structure

Components	Dimensions	Length	Quantity
Angles	1.5” x 1.5” x 0.125”	12.0”	10
Angles	1.5” x 1.5” x 0.125”	9.0”	4
Channels	1.5” x 1.0” x 0.125”	16.5”	2
Channels	1.5” x 1.0” x 0.125”	3.0”	6

The tote is positioned outside the lab to allow environmental factors to directly affect the soil condition. The decimal degree relative to latitude and longitude is obtained from the google maps. The decimal degree is converted to DMS Latitude (49°16’40.1448” N) and Longitude (122°54’50.1156” W) to locate the nearby Weather Canada Station. The weather database available online for the station is used to obtain precipitation and temperature data. Other factors that affect soil corrosion are unchanged as the soil is kept in a tote. If the grillage along with RE and CE would have been buried under the ground, then various factors (such as microorganisms) would affect the grillage corrosion. Thus, to only take into account the macro-environmental factors the grillage is kept in the tote.

(a) (b)

Figure 24: Miniature grillage structure and; (b) tote placed outside the laboratory

A continuous long-term experiment is performed using the ACPS system. The ACPS based protection system is integrated with the off-grid solar energy. The ACPS setup is used to obtain the polarization curve by sweeping potential on the grillage (WE) with reference to the $Cu/CuSO_4$ reference electrode. The Tafel curve is obtained using anodic to cathodic sweep to extract the protection parameters. The protection power based on the extracted parameters (I_{corr} and E_{corr}) is supplied to the grillage structure. The grillage is protected using the protection parameters for 120 minutes and the measurement cycle is repeated to update the protection parameters. The daily average values of I_{corr} and E_{corr} is obtained and correlated with the precipitation and temperature data.

6.2. Results and Discussion

Grillage corrosion depends on the interaction of the metal with the soil. The corrosion in soil is a multi-level process affected by its macro-environment. Macro-environment in-terms of precipitation and temperature will affect soil conditions [30]. As mentioned earlier, the experiment was performed using a miniature grillage structure submerged in soil. The correlation of macro-environmental factors with the electrochemical corrosion values is discussed in this section.

The trend of E_{corr} and the mean temperature is shown in Figure 25. Due to the tote size constraints, the anode and cathode are in close proximity. The formation of rust on the metal surface reduces the corrosion rate over time [20]. As the electrodes are placed in the vicinity, a decreasing trend in E_{corr} is observed for the first half of the experiment. The trend of I_{corr} and the mean temperature is shown in Figure 27. Simultaneous observation of temperature and precipitation is needed. The trend of E_{corr} and I_{corr} with precipitation (variations with respect to time) is shown in Figure 26 and Figure 28 respectively.

The experimental study started in September and is continued during the winter months. Thus, a general decline in daily mean temperature is seen. Additionally, the decrease in temperature would not allow the moisture to evaporate fast-enough from the soil. Hence, current density decreases with an increase in soil moisture content with time. Additionally, the soil retains moisture due to precipitation. A declining trend of I_{corr} is

observed for the majority of the experiment except for the last few data points. The temperature dropped below zero degrees for the last section of the data collection.

For analyzing behavior, the data set is divided into three parts. For the first half of the experiment, the minimal effect of precipitation is observed. The soil is relatively dry during the period and thus, the effect of temperature can be easily observed. An inverse relationship is seen between E_{corr} and the temperature. At data point-3 as the temperature decreases, an increase in E_{corr} is noticed. Similarly, a relative decline in temperature at data point-14 is realized with a slight peak in E_{corr}. Conversely, an increase in temperature (data point-9 and 19), leads to trough in the E_{corr} trend. For the next few data sets, the moisture content of the soil increases due to macro-environment precipitation. A lesser correlation of E_{corr} and temperature is observed for this data set. Negative temperature is recorded for the last few days of the experiment. From Figure 25, it is noticed that the E_{corr} values decline further with the temperature. However, I_{corr} is seen to increase during this period.

As observed by many researchers, corrosion current density depends primarily on the soil moisture [30] [33] [34]. Thus, it can be concluded that the ACPS based system optimizes the protection parameters depending on the environmental conditions. This avoids under-protection and over-protection of the target structure. Being a dynamic corrosion protection system, ACPS allows adjustment of required power consumption. Hence, this system ideally protects the grillage structure.

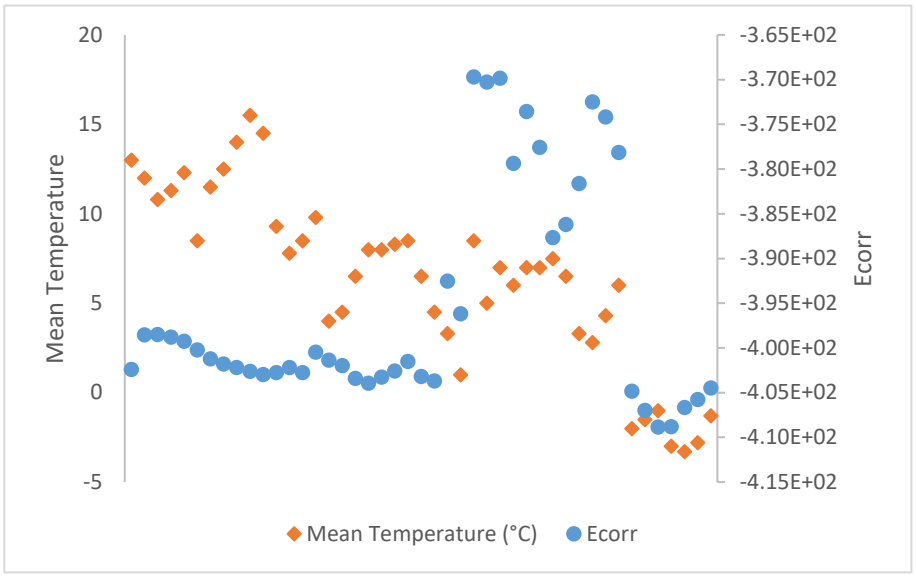

Figure 25: Variation of Ecorr and mean temperature

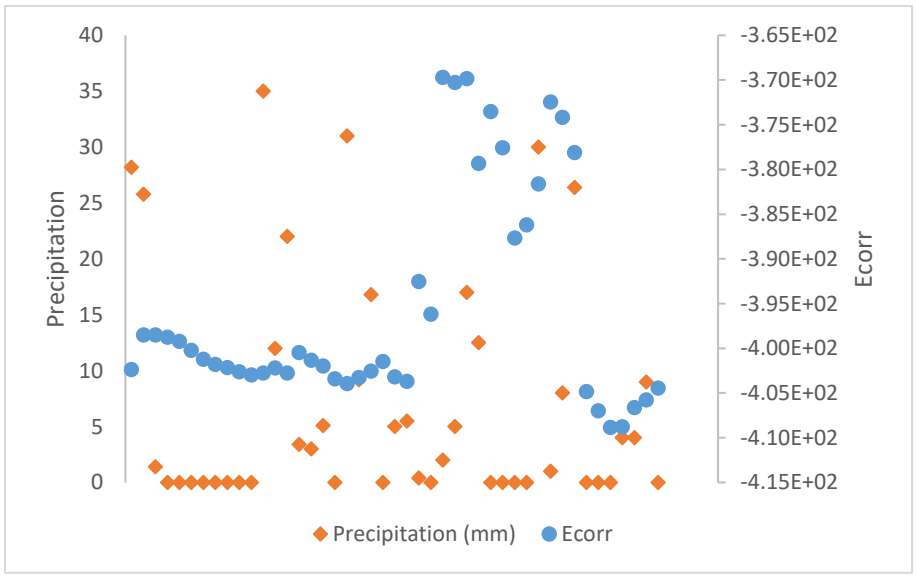

Figure 26: Variation of Ecorr and precipitation

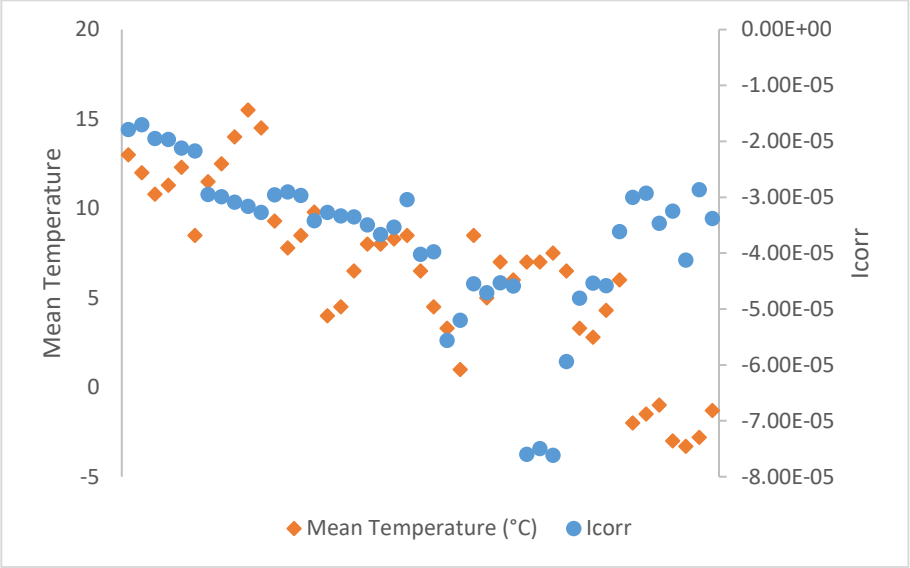

Figure 27: Variation of Icorr and mean temperature

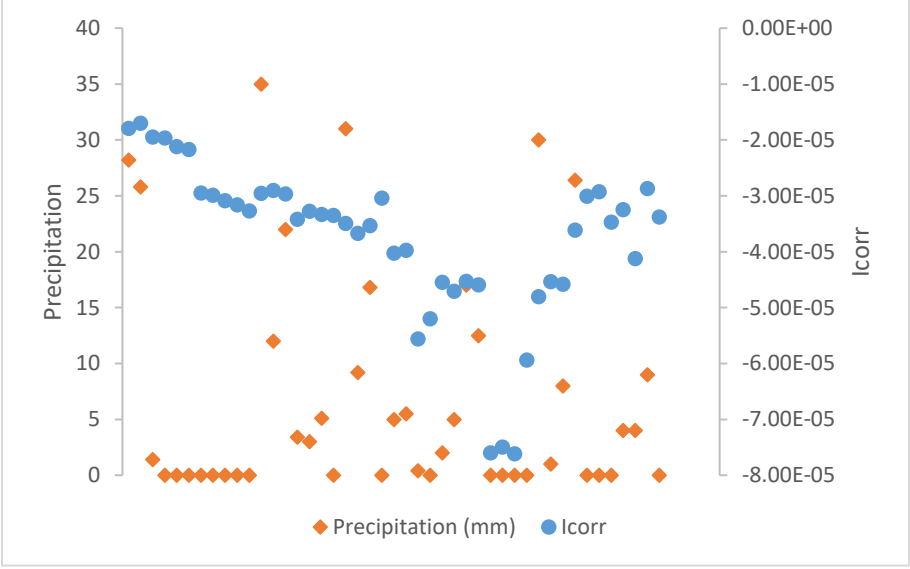

Figure 28: Variation of Icorr and precipitation

Chapter 7.

Conclusions

7.1. Summary

The Adaptive Corrosion Protection System (ACPS), proposed by Patel et al., uses E-Log-I criterion in a feedback loop for cathodic protection of target metal. The ACPS is developed as a stand-alone unit that can diagnose the corrosion status and update the protection parameters using an adaptive loop. Impressed Current Cathodic Protection (ICCP) is another cathodic protection mechanism described in NACE standard practices. The ICCP is a widely used cathodic protection approach that is based on the -0.850V criterion. The novel feedback loop based approach along with the ICCP is used to protect the target metal.

A preliminary analysis is done to validate the ACPS based system in 3% NaCl solution at temperature range from 30 °C to 80°C. A comparative study is performed in a lab environment where the target metal is effectively protected with the corrosion efficiency of 69-100% using the adaptive corrosion protection system. The protection efficiency of ACPS is comparable with the ICCP system. The protection parameters are automatically updated to ensure optimal protection.

The ACPS (current-sourced) system is also compared with the ICCP in different corrosive mediums. Novel hardware and software module using the ACPS feedback-loop mechanism are developed for this research. The extensive comparative analysis is done in 3% NaCl solution at temperatures between 30°C and 80°C. Additionally, the ACPS system is compared with ICCP in different pH mediums of 2 to 12. The study clearly shows the protection efficiency of the stand-alone ACPS unit is comparable to the ICCP mechanism. It also evades the possible human interaction. Unlike the potential based ICCP system, the dynamic ACPS optimizes the protection current to avoid the risk of under and over protection.

The novel hardware and software module of ACPS integrated with off-grid solar energy are used to protect a miniature transmission tower grillage structure. A grillage structure is prepared using A36 steel and is submerged in soil. A long-term continuous

experiment is performed in an uncontrolled environment. Macro-environmental factors are compared with the corrosion parameters. The effect of temperature and precipitation is studied for the dynamic ACPS corrosion protection system. It is concluded that the ACPS adapts well with the changing environmental conditions to avoid under and/or over protection of the target structure. It optimizes power consumption and ideally protects the grillage structure from the uniform corrosion.

In summary, ACPS offers a novel approach to the traditional potential-sourced cathodic corrosion protection system. The standalone ACPS solution is developed and used for this research. The experimentation and validation criteria are identified in coordination with BC Hydro and Powertech Labs.

7.2. Recommendations for Future Work

7.2.1. Size Optimization

The ACPS module prepared for this research can be used to protect actual transmission tower grillages and other infrastructures. The booster unit integrated with the ACPS micro-controller board is capable of high power source and sink. The protection power required is dependent on the surface area of the target structure. Thus, actual grillage will need more power than the metal coupons.

The subsequent step for this research is the in-field implementation of the ACPS. An actual grillage from the BC Hydro transmission tower will be used as a target structure. The field test will validate the power requirement by the booster unit. A comparison of power savings by the dynamic ACPS can be determined from the field test. The anode consumption is observed for the cathodic protection systems. The in-field implementation of ACPS with larger target metal surface area will aid to determine the anode consumption. Though the protection parameters are updated at a user-defined interval, the anode consumption for this approach will allow for cost-benefit analysis for industrial applications.

7.2.2. Repeatability and Reliability

Electrochemical performance of steel depends on its composition. The change in metal properties due to alloying have varying effects on its corrosion. Alloying is generally

done to make steel more corrosion resistant. Apart from iron, steel is also composed of small amounts of molybdenum, chromium, copper and nickel. The chemical composition of the steel determines its electrochemical response in changing environmental conditions. ASTM A36 steel is used in this research. However, other steel composition will have different electrochemical response and further tests should be carried out to understand its behavior.

Additionally, other metallurgical factors also influence corrosion. Impurity, stress, heterogeneity, shape, crystallography, grain-size and its orientation can affect corrosion performance. These factors are altered during the mechanical treatments or subsequent processing such as welding. These processing can create different electrochemical characteristics. Apart from welding, grillage structures are also composed of dissimilar metal pieces such as bolts. The different material will have different corrosion properties then the base metal. Therefore, these factors should be taken into account to study the corrosion behaviour.

Further, corrosion in natural environments has a non-linear behaviour. Due to the complex set of factors that affect corrosion, an experimental design that encompasses these factors in natural setting should be carried out. Apart from uniform corrosion, microorganism induced corrosion is difficult to diagnose. Microorganisms are ubiquitous and are attracted to both anodic and cathodic sites. Thus, monitoring the effects of such factors only using electrochemical methods is insufficient.

Furthermore, often sacrificial anodic protection is used in the marine environment. As 3% NaCl solution as corrosive medium represents sea-water, other such protection mechanisms can be compared with the ACPS. Moreover, constant monitoring to obtain Tafel segment affects the corrosion behaviour. Hence, the recursive sweeping of potential should be optimized.

7.2.3. Integration with the Smart-Grid Infrastructure

The novel stand-alone (current-sourced) ACPS system offers continuous corrosion monitoring and protection mechanism. Hence, it can be used as an independent protection system that can be directly integrated with a smart-grid communication network (Figure 29). Corrosion monitoring can be done directly from the utility company's control

room. The ACPS system allows to report corrosion status of the infrastructure and send alert signals to the control room in case of any abnormal environmental effect on the smart-grid infrastructure. Such amalgamation with the smart-grid network results in high reliability of the grid performance by avoiding blackouts due to any structural failure.

Moreover, multiple grillage structures can be protected by deploying various ACPS units. Resin.io makes it easy to deploy code to fleets of connected devices. If these features are integrated with the ACPS, the units can be located on a map (as shown in Figure 30) from the control room. This will allow location specific corrosion monitoring. These features will also enable data collection and such repository development will aid site specific data analysis. Furthermore, further developments using such system may allow monitoring data from mobile devices. This automated corrosion monitoring and protection system enables risk management of the infrastructure (Figure 31).

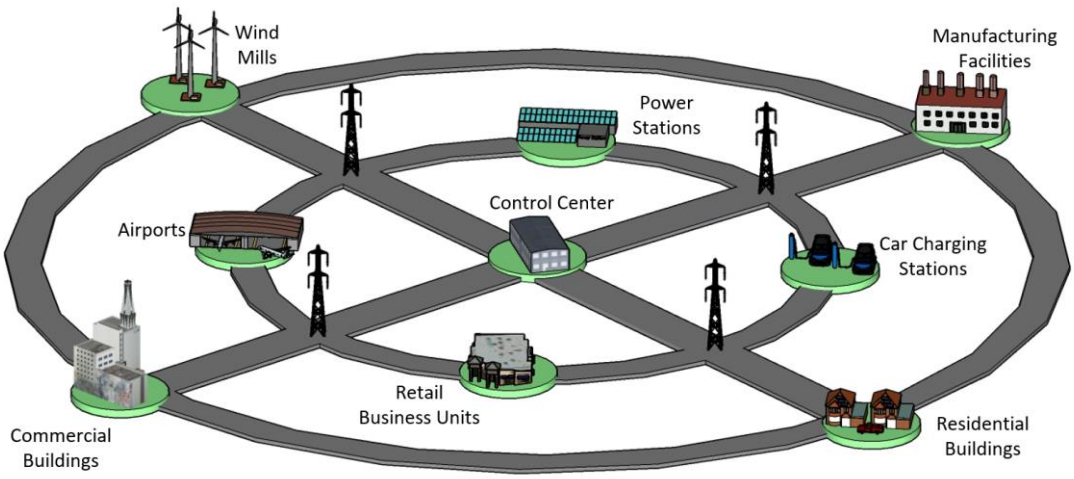

Figure 29: Smart-grid network

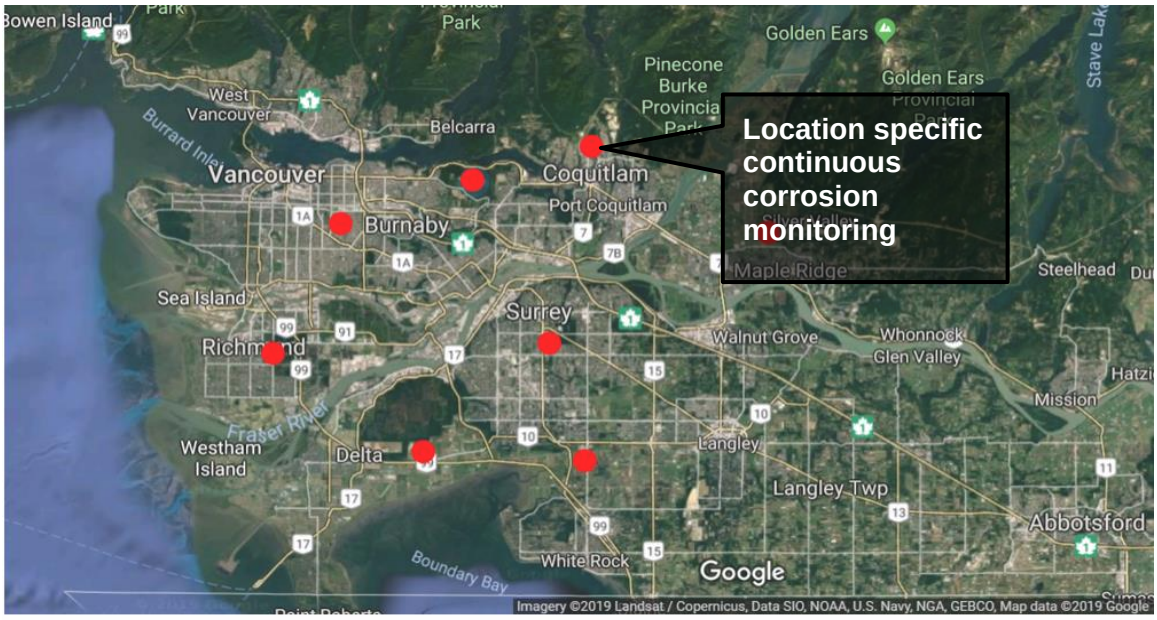

Figure 30: Location specific corrosion monitoring using ACPS

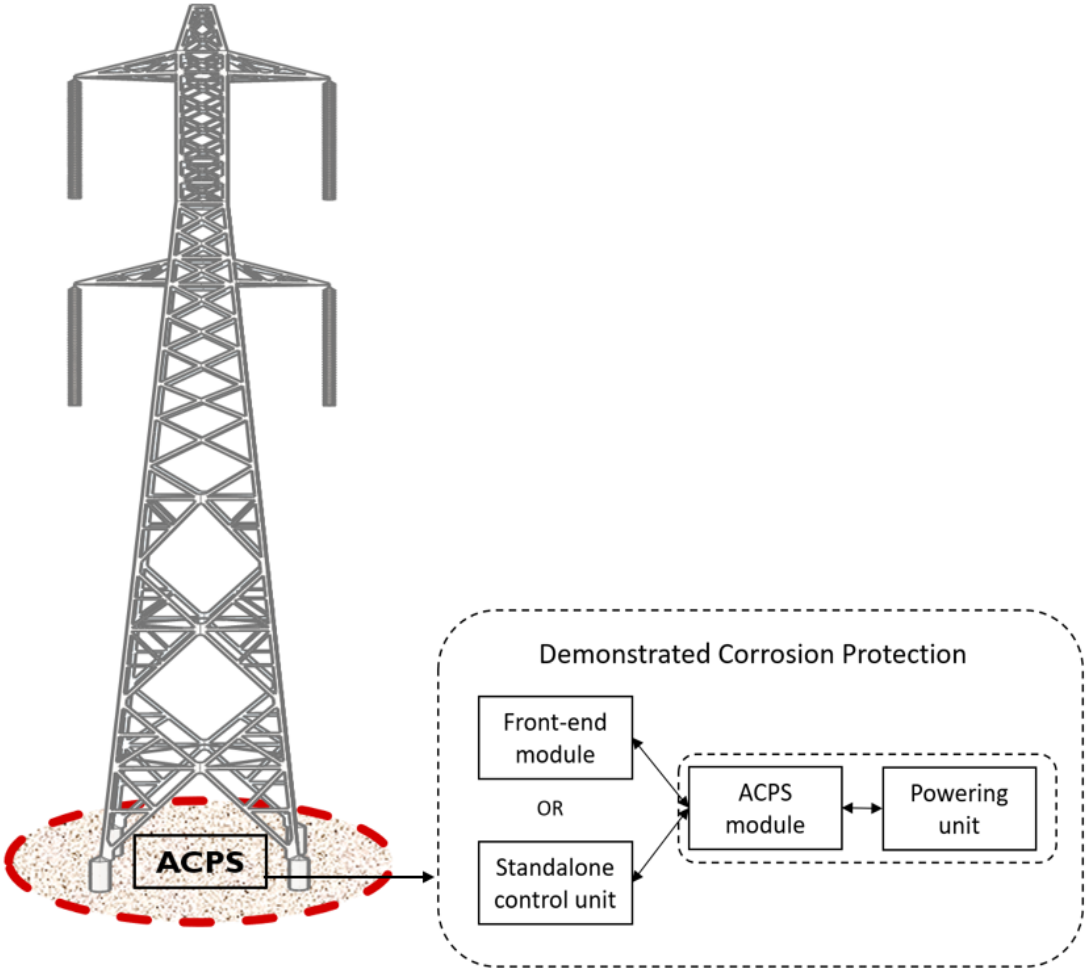

Figure 31: Effective solution for continuous corrosion monitoring and protection

References

[1] National Association of Corrosion Engineers, "impact.nace.org," International Measure of Prevention, Application, and Economics of Corrosion Technologies Study, [Online]. Available: http://impact.nace.org/documents/summary-supplement.pdf. [Accessed 15 May 2019].

[2] U.S. Department of Energy, "www.energy.gov," [Online]. Available: https://www.energy.gov/sites/prod/files/2015/09/f26/QER_AppendixC_Electricity.pdf. [Accessed 10 May 2019].

[3] K. Knutson, "www.tdworld.com," [Online]. Available: https://www.tdworld.com/transmission/drivers-and-challenges-transmission-investment. [Accessed 20 April 2019].

[4] H. . Kihira, "Systematic approaches toward minimum maintenance risk management methods for weathering steel infrastructures," *Corrosion Science,* vol. 49, no. 1, pp. 112-119, 2007.

[5] F. Plumptre, M. Nagpal, X. Chen and M. Thomson, "Protection of EHV transmission lines with series compensation: BC hydro's lessons learned," in *2009 62nd Annual Conference for Protective Relay Engineers*, 2009.

[6] P. Taheri, A. Mansouri and M. Zamanzadeh, "Numerical Simulation of Cathodic Protection Systems for Transmission Tower with Grillage-Type Foundations," in *NACE International Corrosion Conference*, 2016.

[7] E. E. Stansbury and R. A. Buchanan, Fundamentals of electrochemical corrosion, ASM International, 2000.

[8] D. A. Jones, Principles and prevention of corrosion, Macmillan, 1996.

[9] L. Veleva and R. D. Kane, ASM Handbook: Atmospheric Corrosion, Corrosion: Fundamentals, Testing, and Protection, vol. 13A, ASM International, 2003.

[10] J. Rodriguez, F. Hernandez and J. Gonzalez, "The effect of environmental and meteorological variables on atmospheric corrosion of carbon steel, copper, zinc and aluminium in a limited geographical zone with different types of environment," *Corrosion Science,* vol. 4, no. 45, pp. 799-815, 2003.

[11] N. Perez, Electrochemistry and corrosion science, vol. 412, Boston: Kluwer Academic Publishers, 2004.

[12] M. Kutz, Handbook of environmental degradation of materials, William Andrew, 2018.

[13] *Standard Practice on Control of External Corrosion on Underground or Submerged Metallic Piping Systems,* Houston, Texas: NACE, 2013.

[14] J. N. Patel, A. . Chang, H. . Shahbazbegian and B. . Kaminska, "Adaptive Corrosion Protection System Using Continuous Corrosion Measurement, Parameter Extraction, and Corrective Loop," *International Journal of Corrosion,* vol. 2016, no. , pp. 1-11, 2016.

[15] A. J. Bard, L. R. Faulkner, J. Leddy and C. G. Zoski, Electrochemical methods: fundamentals and applications, vol. 2, New York: Wiley.

[16] K. V. Rybalka, L. A. Beketaeva and A. D. Davydov, "Cathodic Component of Corrosion Process: Polarization Curve with Two Tafel Portions," *Russian Journal of Electrochemistry,* vol. 54, no. 5, pp. 456-458, 2018.

[17] E. McCafferty, "Validation of corrosion rates measured by the Tafel extrapolation method," *Corrosion Science,* vol. 47, pp. 3202-3215, 2005.

[18] E. Lopez-Baltazar and J. Genesca, "Laboratory Corrosion Investigation of Some CP Criteria," in *NACE Corrosion*, 2009.

[19] S. D. Cramer, B. S. Covino, G. R. Holcomb and M. Ziomek-Moronz, Conventions and Definitions in Corrosion and Oxidations, vol. 13A, ASM International, 2003, pp. 1002-1008.

[20] V. Cicek, Cathodic Protection: Industrial Solutions for Protecting against Corrosion, John Wiley & Sons, 2013.

[21] R. A. Gummow, "Cathodic Protetcion Criteria - A Critical Review of NACE Standard RP-01-69," *Material Performance,* vol. 57, no. 1, p. 33, 2018.

[22] E. A. Noor and A. H. Al-Moubaraki, "Influence of Soil Moisture Content on the Corrosion Behavior of X60 Steel in Different Soils," *Arab J Sci Eng,* vol. 39, pp. 5421-5435, 2014.

[23] C. C. Lin and C. X. Wang, "Correlation between accelerated corrosion tests and atmospheric corrosion tests on steel," *Journal of Applied Electrochemistry,* vol. 35, pp. 837-843, 2005.

[24] F. M. Mulimbayan and M. G. Mena, "Investigation of the Effects of Solution Temperature on the Corrosion Behavior of Austenitic Low-Nickel Stainless Steels in Citric Acid using Impedence and Polarization Measurements," *MATEC Web of Conferences,* vol. 27, no. 02006, 2015.

[25] X. H. Nie, X. G. Li, C. W. Du and Y. F. Cheng, "Temperature dependence of the electrochemical corrosion characteristics of carbon steel in a salty soil," *J Appl Electrochem,* vol. 39, pp. 277-282, 2009.

[26] H. Mohebbi and C. Q. Li, "Experimental Investigation on Corrosion of Cast Iron Pipes," *International Journal of Corrosion,* 2011.

[27] A. Popova, "Temperature effect on mild steel corrosion in acid media in presence of azoles," *Corrosion Science,* vol. 49, pp. 2144-2158, 2007.

[28] D. G. Li, Y. R. Feng, Z. Q. Bai, J. W. Zhu and M. S. Zheng, "Influence of temperature, chloride ions and chromium element on the electronic property of passive film formed on carbon steel in bicarbonate/carbonate buffer solution," *Electrochimica Acta,* vol. 52, pp. 7877-7884, 2007.

[29] S. Takasaki and Y. Yamada, "Effects of temperature and aggressive anions on corrosion of carbon steel in potable water," *Corrosion Science,* vol. 49, pp. 240-247, 2007.

[30] I. S. Cole and D. Marney, "The science of pipe corrosion: A review of the literature on the corrosion of ferrous metals in soils," *Corrosion Science,* vol. 56, pp. 5-16, 2012.

[31] Y. H. Wu, T. M. Liu, S. X. Luo and C. Sun, "Corrosion characteristics of Q235 steel in simulated Yingtan soil solutions," *Materialwissenschaft und Werkstofftechnik,* vol. 41, no. 3, pp. 142-146, 2010.

[32] A. Benmoussa, M. Hadjel and M. Traisnel, "Corrosion behavior of API 5L X-60 pipeline steel exposed to near-neutral pH soil simulating solution," *Materials and corrosion,* vol. 57, no. 10, pp. 771-777, 2006.

[33] S. K. Gupta and B. K. Gupta, "The critical soil moisture content in the underground corrosion of mild steel," *Corrosion Science,* vol. 19, no. 3, pp. 171-178, 1979.

[34] J. N. Murray and P. J. Moran, "Influence of moisture on corrosion of pipeline steel in soils using in situ impedence spectroscopy," *Corrosion,* vol. 45, no. 1, pp. 34-43, 1989.

[35] M. Norin and T. G. Vinka, "Corrosion of carbon steel in filling material in an urban environment," *Materials and corrosion,* vol. 59, no. 9, pp. 641-651, 2003.

[36] R. Akkouche, C. Remazeilles, M. Jeannin, M. Barbalat, R. Sabot and P. Refait, "Influence of soil moisture on the corrosion process of carbon steel in artificial soil: Active area and differential aeration cells," *Electrochimica Acta,* vol. 213, pp. 698-708, 2016.

[37] C. N. Neale, J. B. Hughes and C. H. Ward, "Impacts of unsaturated zone properties on oxygen transport and aquifer reaeration," *Groundwater,* vol. 38, no. 5, pp. 784-794, 2000.

[38] American Water Works Association, *Polyethylene Encasement for Ductile-Iron Pipe Systems,* AWWA, 2010.

[39] J. G. Kim and Y. W. Kim, "Cathodic protection criteria of thermally insulated pipeline buried in soil," *Corrosion Science,* vol. 43, no. 11, pp. 2011-2021, 2001.

[40] M. Sancy, Y. Gourbeyre, E. M. Sutter and B. Tribollet, "Mechanism of corrosion of cast iron covered by aged corrosion products: Application of electrochemical impedence spectrometry," *Corrosion Science,* vol. 54, no. 4, pp. 1222-1227, 2010.

[41] J. B. Bushman and T. E. Mehalick, "Statistical analysis of soil characteristics to predict mean time to corrosion failure of underground metallic structures. In effect of soil characteristics on corrosion," *ASTM International,* 1989.

[42] C. Ferreira, J. A. Ponciano, D. S. Vaitsman and D. V. Perez, "Evaluation of the corrosivity of the soil through its chemical composition," *Science of the total environment,* vol. 388, no. 1-3, pp. 250-255, 2007.

[43] R. W. Revie, Corrosion and Corrosion Control, Hoboken, NJ, USA: John Wiley & Sons, 2008.

[44] D. Mendoza, R. Perez and A. Aguilar, "Cathodic Protection Behavior of API X-52 And API X-65 Steels Burried in Natural Soil," in *NACE Corrosion*, 2011.

[45] A. Oni, "Effects of cathodic overprotection on some mechanical properties of a dual-phase low alloy steel in sea water," *Construction and Building Materials,* vol. 10, no. 6, pp. 481-484, 1996.

[46] AZoM, "AZO Materials," 2012. [Online]. Available: https://www.azom.com/article.aspx?ArticleID=6117. [Accessed March 2019].

[47] "Raspberry Pi Foundation," [Online]. Available: https://www.raspberrypi.org/.

[48] A. Trivedi, S. Bhadauria and R. Sengar, "Analytical Study of Influence of pH and Weight-loss on Steel Corrosion Embedded in Reinforced Concrete: A Review Paper," *International Journal of Advanced Science and Technology,* vol. 91, pp. 59-70, 2016.

[49] Z. Muslim and A. Abbas, "The Effects of pH and Temperature on Corrosion Rate Stainless Steel 316L Used as Biomaterial," *International Journal of Basic and Applied Science,* vol. 4, pp. 17-20, 2015.

[50] B. Pijanowski and I. Mahmud, "A Study of the Effects of Temperature and Oxygen Content on the Corrosion of Several Metals," *Institute of Ocean Science and Engineering at the Catholic University of America,* Vols. Report 69-2, 1969.

[51] N. Kairi and J. Kassim, "The Effect of Temperature on the Corrosion Inhibition of Mild Steel in 1M HCl Solution by Curcuma Longa Extract," *International Journal of Electrochemical Science,* vol. 8, pp. 7138-7155, 2013.

[52] A. Malik, P. Kutty, N. Siddiqi, I. Andijani and S. Ahmed, "The Influence of pH and Chloride Concentration on the Corrosion Behavior of AISI 316L Steel in Aqueous Solutions," *Corrosion Science,* vol. 33, pp. 1809-1827, 1992.

[53] E. Phelps and D. Vreeland, "Corrosion of Austenitic Stainless Steel in Sulfuric Acid," in *NACE Annual Conference*, 1957.

[54] J. Truman, "The Influence of Chloride Content, pH and Temperature of Test Solution on the Occurrence of Stress Corrosion Cracking with Austenitic Stainless Steel," *Corrosion Science,* vol. 17, pp. 737-746, 1977.

[55] B. Beverskog and I. Puigdomenech, "Revised Pourbaix Diagrams for Iron at 25-30C," *Corrosion Science,* vol. 38, pp. 2121-2135, 1996.

Appendix. System Level Design

An effective standalone corrosion protection system is designed and presented in this thesis. The workflow of the ACPS interface is shown in Figure 32. Before executing the program, user-input values of Tafel measurement and chronopotentiometry experiment is recorded. When the experiment is executed, the Open Circuit Potential is measured. Consequently, the Tafel response is obtained according to the user-input Tafel measurement values. Protection variables are extracted from this response. The system is then switched over to the protection mode. The plot of both Tafel measurement and protection mode can be observed through the GUI. The interface screen of the ACPS is shown in Figure 33. Additionally, the ACPS microcontroller board is shown in Figure 34. The overall implementation of the entire system in its totality was done with the help of others working on this project. This project is developed under Mitacs multi-year program in collaboration with the industry partners. The project report submitted by other team member highlights in more detail the specifics of the firmware, interface and hardware[1]. The author of this thesis managed the system level solution by collaborating effectively with all stakeholders.

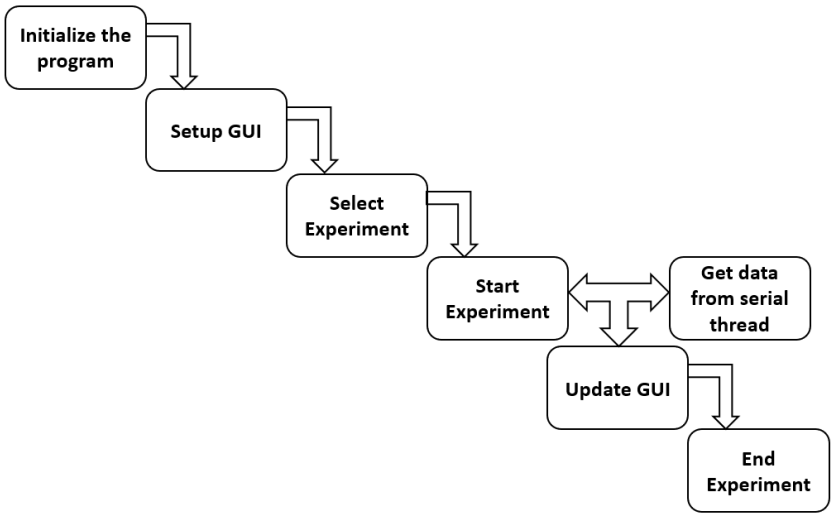

Figure 32: ACPS interface workflow

[1] A. Chowdhury, "Adaptive Corrosion Protection System for Smart-Grid Applications," A project report submitted to Simon Fraser University library in partial fulfillment of the requirements for the degree of Master of Engineering, 2019.

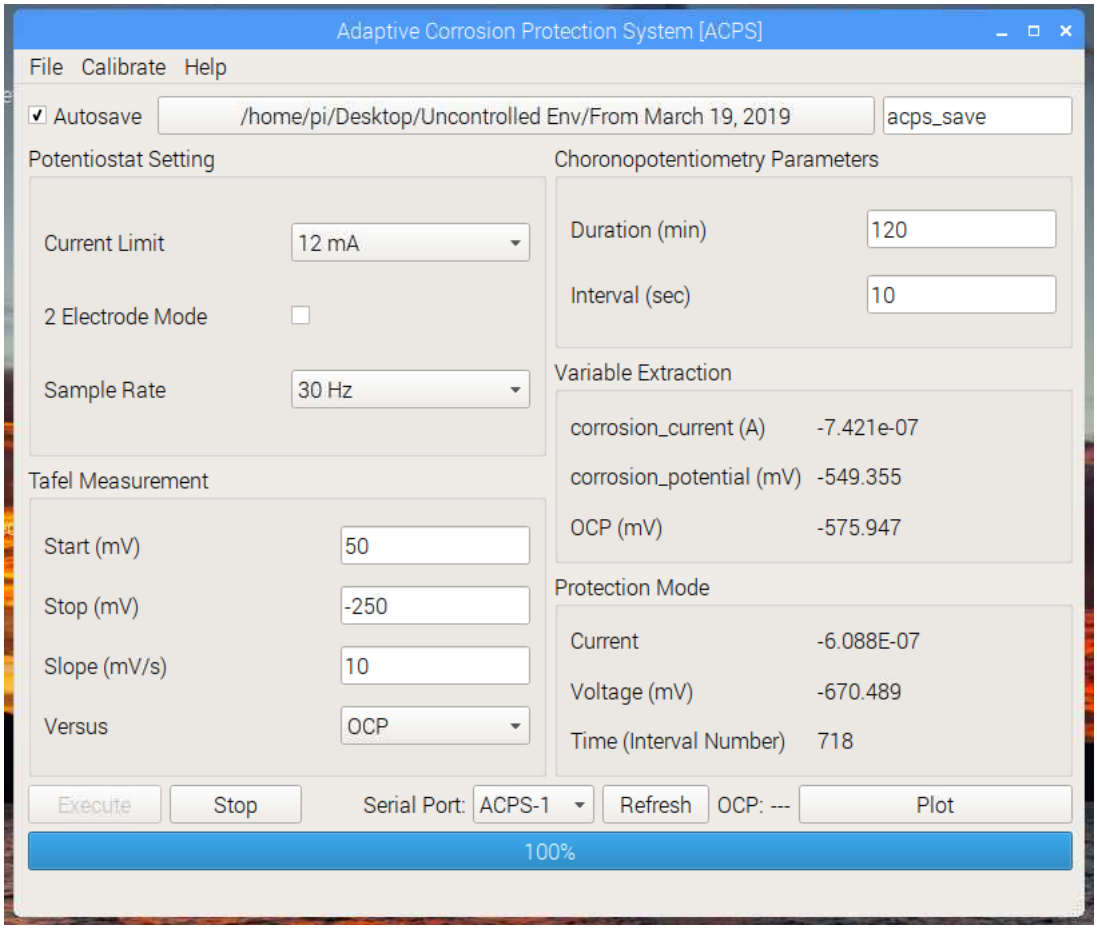

Figure 33: ACPS interface

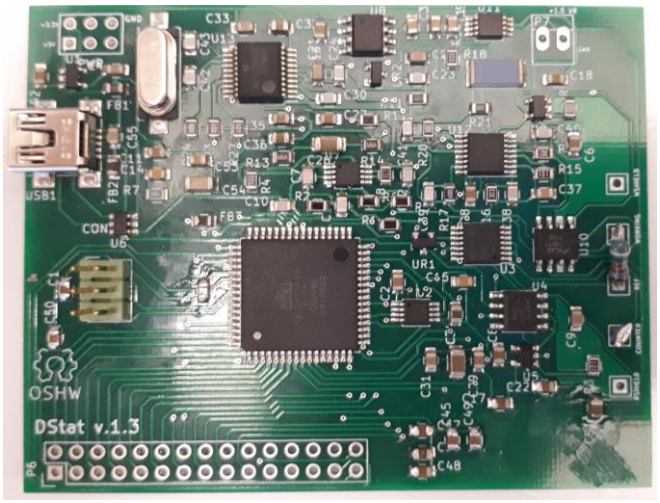

Figure 34: ACPS microcontroller board